

CFD SIMULATION OF TURBULENT HEAT TRANSFER IN AN AGITATED VESSEL

Thesis submitted in partial fulfillment of the requirements for the award of
the degree of

MASTER OF ENGINEERING

IN

THERMAL ENGINEERING

Submitted by:

HARWINDER SINGH

Reg. No-821183002

July,2014

Under the Supervision of

Dr. Avinash Chandra
Assistant Professor
Chemical Engineering Department
Thapar University

Dr. Vikas Kumar Sangal
Assistant Professor
Chemical Engineering Department
Thapar University



DEPARTMENT OF MECHANICAL ENGINEERING
THAPAR UNIVERSITY
PATIALA-147004, INDIA,

DECLARATION

I hereby certified that the work which is being presented in dissertation entitled, “ **CFD SIMULATION OF TURBULENT HEAT TRANSFER IN AN AGITATED VESSEL**” in partial fulfillment of requirements for the award of the degree of Master of Engineering in Mechanical Engineering with specialization in **THERMAL ENGINEERING** submitted in **Mechanical Engineering Department of Thapar University, Patiala**, is an authentic record of my own work carried out under the supervision of **Dr. Avinash Chandra** and **Dr. Vikas Kumar Sangal**. The work refers other researcher’s works which are duly listed in the references section.

The matter presented in this thesis has not been submitted for the award of any other degree of this or any other university.

Date: 17/July/2014

Place: Patiala



HARWINDER SINGH

821183002

There is to certify that above statement made by the candidate is correct and true to the best of our knowledge.



Dr. Avinash Chandra

Assistant Professor

Department of Chemical Engineering

Thapar University, Patiala



Dr. Vikas Kumar Sangal

Assistant Professor

Department of Chemical Engineering

Thapar University, Patiala

Countersigned by




Dr. Ajay Batish

Professor & Head of Department

Department of Mechanical Engineering

Thapar University, Patiala



Dr. S.K. Mohapatra

Dean of Academic Affairs

Thapar University, Patiala

ACKNOWLEDGEMENT

My years of Post graduate study are finally nearing completion. This is the opportune moment to Acknowledge all who have crossed my path during the journey and contributed directly or indirectly to reaching the light at the end of the tunnel.

Undoubtedly, my supervisors, **Dr. AVINASH CHANDRA** and **Dr. VIKAS KUMAR SANGAL**, Assistant Professors of Chemical Engineering Department, THAPAR UNIVERSITY , Patiala, deserve to be at the top of the list. It was an excellent opportunity to work under the tutelage of two stalwarts of Chemical engineering. These years have been helpful for my academic progress. I sincerely thank them for their kind guidance, helpful suggestions, encouragement and confidence in me. The fruitful discussions with him throughout the research work were a great help for the successful completion of the present work.

It is a great pleasure to thank the authorities of Thapar University, Patiala for providing this opportunity to carry out my research work successfully.

I owe sincere and earnest thankfulness to my family members who enthused, encouraged and fully supported me for every trial that comes my way..I acknowledge my sincere thanks to all my friends for providing the companionship and making my stay at Thapar University, Patiala pleasant and joyful. Last but not the least, To God the father of all, I thank for the strength that keeps me standing and for the hope that keeps me believing that this affiliation would be possible and more interesting.

HARWINDER SINGH

TABLE OF CONTENTS

TITLE	PAGE NO.
Abstract	i
List of figures	ii
List of tables	iii
Nomenclature	iv
CHAPTER 1	
1. INTRODUCTION	1
CHAPTER- 2	
2. LITERATURE REVIEW	5
CHAPTER- 3	
3. MATHEMATICAL MODELLING	15
3.1 Problem Statement	15
3.2 Geometrical Configuration	16
3.3 Governing Equations	17
3.4 Boundary Conditions	18
3.5 Some Dimensionless Groups	18
3.5.1 Reynold Number	18
3.5.2 Power Number	18
3.5.3 Nusselt Number	19
CHAPTER- 4	
4. NUMERICAL METHODOLOGY	20
4.1 A Brief Introduction to CFD	20
4.1.1 Pre-Processor	21

4.1.2	Processor	21
4.1.3	Post Processor	22
4.2	Numerical Methodology	22
4.3	Simulated Geometry	23
4.4	Rotating Co-ordinate System	25
4.5	Grid Generation	25
4.6	Turbulence Model	27
4.6.1	Standard k- Turbulence Model	28
4.6.2	k- Turbulence Model	29
4.6.3	Shear Stress Model	29
CHAPTER-5		
RESULTS AND DISCUSSION		30
5.1	Validation of the Present Work	30
5.1.1	Axial Velocity Comparison	30
5.1.2	Radial Velocity Comparison	31
5.1.3	Tangential Velocity Comparison	32
5.2	Flow Field Analysis	32
5.2.1	Velocity	32
5.2.2	Pressure	37
5.3	Heat Transfer	38
5.3.1	Isotherm	38
5.4	Average Nusselt Number	41
CHAPTER-6		
CONCLUSION AND FUTURE SCOPE		43
6.1	Conclusion	43
6.2	Future Scope	43

ABSTRACT

Blending and mixing is an important unit operation in process industries. It has broad spectrum of applications ranging from concrete mixing to polymer processing including cosmetics, paints, food stuff, etc. The quality of final product is depends upon the degree of mixing, hence, it is the important area for research and industrial development.

The present work is aiming to explore flow and heat transfer characteristics in an agitated vessel in the turbulent flow regime using CFD simulation. ANSYS Fluent is used as a solver to simulate flow and heat transfer in agitated vessel. A pitched blade turbine with six blades at 45° has been used for the study. The turbine placed concentrically in a cylindrical vessel with flat top and bottom. The cylindrical vessel is subjected to uniform constant wall temperature(jacketed vessel). The Reynolds number of 7.2×10^4 has been chosen for present study. For heat transfer study six values of Prandtl number have been taken as 0.71,7,20,30,40 and 50.

The flow dynamics shows that the velocity near the turbine is very high as compare to vessel surfaces in the horizontal plane and in the vertical plane it is maximum below the turbine. The pressure was found minimum near the impeller and maximum at cylindrical walls. The heat transfer simulation shows that the temperature gradient is small and this gradient further reduces with increasing the Prandtl number and the almost uniform temperature profile obtained at Prandtl number 50 at Reynolds number $=7.2 \times 10^4$. Overall, the present study shows that the degree of thermal mixing increases with increasing Prandtl number. The overall heat transfer also increases with increasing Prandtl number and it shows functional dependency on Prandtl number.

LIST OF FIGURES

Figure No.	Description	Page No.
1.1	Typical arrangement for a mechanical agitated vessel	2
1.2	Flow pattern for an Axial flow impeller	3
1.3	Flow pattern for a Radial flow impeller	3
1.4	Different types of Heat transfer equipments for mixing	4
3.1	Schematic Diagram of investigated agitated Tank	15
4.1	Schematic Presentation of CFD	21
4.2	Simulated geometry of the agitated vessel & impeller	24
4.3	Grid for Vessel and impeller(shaded view)	26
4.4	Grid for Vessel and impeller(wire frame)	27
5.1	Axial velocity at horizontal location $y=88$	30
5.2	Radial velocity at horizontal location $y=88$	31
5.3	Tangential velocity at horizontal location $y=88$	32
5.4	Location of different planes	33
5.5	Axial velocity contours at different cross-section of the vessel	34
5.6	Radial velocity contours at different cross-section of the vessel	35
5.7	Tangential velocity contours at different cross-section of the vessel	36
5.8	Pressure contours at different cross-section	37

5.9	Temperature Profile for $Pr = 0.71$	38
5.10	Temperature Profile for $Pr = 0.7$	39
5.11	Temperature Profile for $Pr = 20$	39
5.12	Temperature Profile for $Pr = 30$	40
5.13	Temperature Profile for $Pr = 40$	40
5.14	Temperature Profile for $Pr = 50$	41
5.15	Average Nusselt Number	42

LIST OF TABLES

Figure No.	Description	Page No.
3.1	Dimensional data for the agitated vessel & impeller	16
3.2	Fluid Properties and other important parameters	16

NOMENCLATURE

H	Vessel height, m
T	Diameter of the vessel, m
C	Impeller off-bottom clearance, m
C_p	Specific heat, J/(kg·K)
D	Impeller diameter, m
w	Width of blade, m
t	Thickness of blade, m
g	Gravitational acceleration, m/s^2
h	Heat transfer coefficient, $W/(m^2K)$
k	Thermal conductivity, $W/(m-K)$
n	number of blades
N	Impeller rotational speed, rev/s
P_i	Impeller power required
r	Radial distance of vessel
N_p	Power number of impeller,
P	Pressure, N/m^2
t	Time-averaged component of pressure, N/m^2
T_w	Wall Temperature, °C
T_f	Fluid Temperature, °C
Re	Reynolds number

Nu	Nusselt number,
Pr	Prandtl number
	Density, kg/m^3
μ	Dynamic viscosity, kg/ms

CHAPTER 1

INTRODUCTION

The mixing is an unit operations encountered in almost all process industries such as drugs & foods, fine chemicals, water treatment, polymers, manufacture of paints & detergents, purification of industrial and household waste, pharmaceuticals, etc (Ciofalo et al., 1996).

The quality of finished product is also depends on the degree of mixing of the fractional components of the product. Proper mixing of components provides good quality products and homogeneity of materials. Undoubtedly, the good quality of products turned up in to economical gains. However, inefficient mixing leads to poor quality products. It is reported that the mixing process in the agitated vessel lead to loss US\$10 billion per year due to the lack of fundamental knowledge and non-optimal energy utilizations (Smith et al., 1990).

The agitation process is a common operation to effect distribution, intermingling, & homogeneity of matter. It is term as mixing when the goal is blending and homogeneity is desirable. Other processes such as reaction, mass transfer (includes solubility and crystallization), heat transfer and dispersion, are also promoted by agitation. The agitation is accomplished by a variety of equipments. Mixing is done by rotating impeller in vertical cylindrical vessel. Impeller rotations produces two type of flow pattern in the agitated vessel namely laminar and turbulent flow. The very high rotation of the impeller produces turbulence in the vessel. The flow pattern depends on the operating value of the Reynolds number.

The agitated vessel may be of different shapes like, flat bottom, dished bottom, conical bottom or spherical bottom A typical configuration of a mechanically agitated vessel is illustrated in figure

1.1. The principle components of a mechanically agitated vessel consist of a vessel, baffles and impeller(s).

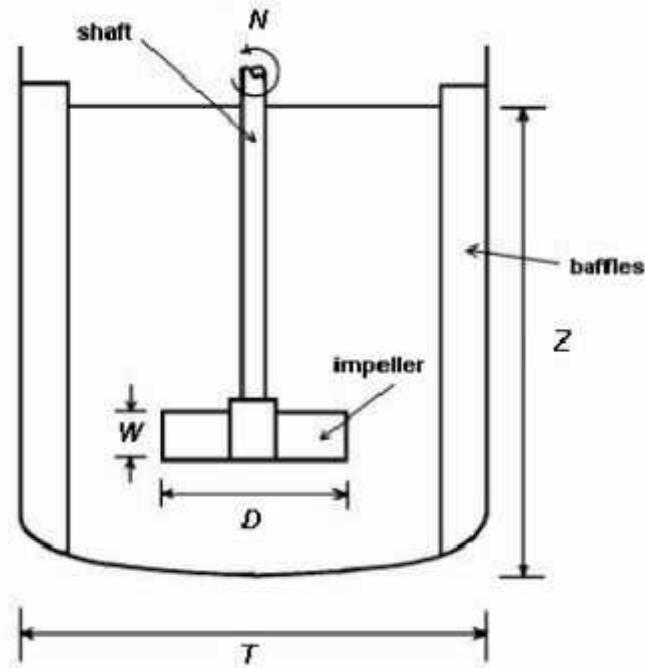


Figure 1.1 Typical arrangement for a mechanical agitated vessel (Harnby et al., 1985).

The mixing impellers can be classified into two broad categories – axial flow impellers and radial flow impellers (Oldshue, et al., 1983) as shown in figure 1.2 and 1.3. The Axial flow impellers produce a principal direction of discharge which coincides with the axis of impeller rotation. As shown in figure 1.2, a single circulation loop emerges from lower surface of the impeller, toward the tank bottom, up side walls, to the upper part of the tank, and back to the impeller along the impeller shaft to the core of the tank. Pitched blade turbine is the example of axial flow impeller. Depending on the direction of rotation, this axial flow can be upwards or downwards. These axial flow impellers produce a large circulation with more flow per horsepower than radial flow impellers and are generally suited to flow controlled operations, such as solid suspension and mixing of miscible liquids (Harnby et al., 1985).

However, radial flow impellers create a strong flow outwards from the impeller that is normal to the axis of impeller rotation as shown in figure 1.3. This flow characteristic creates two circulation zones, above and below the impeller. The strong discharge flow from radial impellers generates high shear stresses and turbulence. The Rushton and anchor turbine are the examples of radial flow impellers.

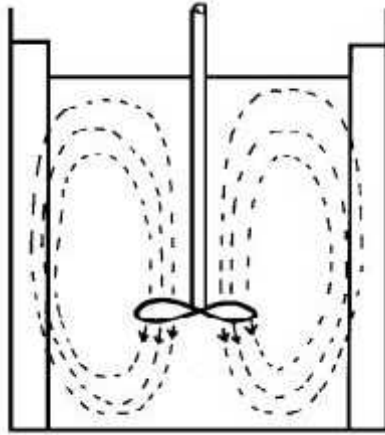


Figure. 1.2 Flow pattern for a axial flow impeller (Harnby et al., 1985).

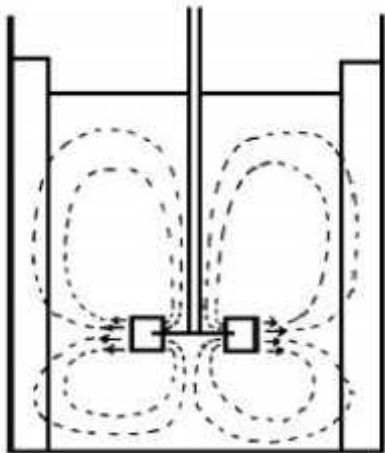


Figure 1.3 Flow pattern for a radial flow impeller (Harnby et al., 1985).

The internal features, including the vessel itself, are considered as a whole, that is, as the agitation system. The force applied by impeller develop overall circulations and bulk flow in the vessel (McCabe et. al., 2005).

Most of the process mixing/agitation operation are also involve with heat transfer operation. Heat can be transfer in agitated vessels either through an external jacket on the vessel or by internal coils as shown in figure 1.4. Jacketed vessels are relatively easy to fabricate and economical but offer a constrained heat transfer area (Oldshue et al.,1983). In contrast, the large heat transfer surface for a given volume of process fluid is obtained by using helical coils and vertical tubes. However, the fabrication and maintenance is very difficult in case of helical coils. Furthermore, the vertical tube arrangement act as baffles, producing top-to- bottom circulation in addition to heat transfer (Yang et al., 2013).

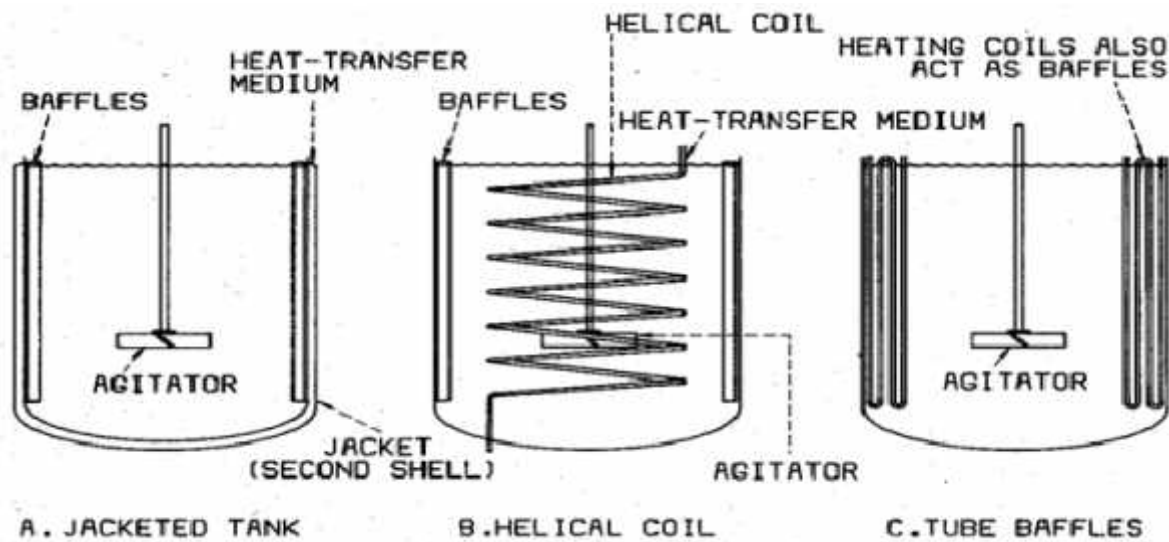


Figure 1.4 Different types of Heat transfer equipments for mixing (Oldshue et al.,1983).

CHAPTER 2

LITERATURE REVIEW

The flow and heat transfer in an agitated vessel have been discussed by many authors both experimentally (Yianneskis, M., 1987; Armenante, et al., 1997; Nere et al., 2003; Nagata, S., 1975 etc.) and numerically (Yeoh, S.L., 2004; Bakker et al, 1996; Barbara et al., 2004; Yang et al., 2013, etc). In this chapter, the available relevant literature on the experimental and numerical studies have been reviewed and presented here.

Chtourou et al.,2014 had worked on the square design of agitated vessel. A standard Rushton turbine had been used. The steady state flow was simulated by MRF approaches. They had been presented the average velocity and turbulent kinetic energy characteristics at different planes. The maximum average speed was predicted in the impeller region. The almost constant speed was observed in the region between the turbine blades tips and the tank walls. The comparison of CFD results with experimental measurements was presented with good agreement.

Yang et al.,2013 had worked on (DES),SRF and LES methods of the liquid-phase turbulent flow in an unbaffled agitated tank. The tank is equipped with a six-bladed 45° pitched blade turbine.. The commercial code Fluent was used for simulations. Results obtained by DES were compared with experimental Laser Doppler velocimeter (LDV) data and also with the predictions obtained by LES. The numerical results of mean velocity and turbulent kinetic energy profiles as well as the power consumption are in good agreement with the LDV data. LES was found accurate than the DES.

Ghotli et al.,2013 had studied the mixing performance in a stirred tank by using number of parameters. Input parameters such as impeller design, power number, flow pattern, number of impellers, and dispersed phase volume fraction were studied in addition to physical properties of phases such as viscosity and density.

Pasquim et al.,2013 had examined the behavior of the three dimensional flow of water. An agitated tank equipped with a Rushton Turbine was used. ANSYS CFX version 13 software is used for the numerical solution of the governing equations. It was predicted that the imperfection of industrial mixing equipment and inappropriate operating conditions adversely affect process performances, hence this area needs more capacious, systematic and thoughtful studies.

Driss et al., 2012 had studied the effect of multiple Rushton impellers. The velocity components and viscous dissipation rate was reported. These results shows that the multi-impellers systems are elementary to decrease the weaken zones in each stirred tanks. The experimental results are compared with numerical results and good agreement validates the numerical method.

Karimi et al., 2012 had focused on the effects of grid schemes and turbulence models in the CFD modeling of stirred tanks. The economical grid was found by examining the dimensionless wall distance and the skewness of elements. Three categories of turbulence models were compared for prediction of flow pattern,. The grid sensitivity study reported that the quality of control volumes in the bulk and near the wall regions are significant for obtaining the consistent solutions. RANS based models are more efficient for the prediction of velocity components and the turbulent quantity,

Karcz, et al.,2012 had predicted the effects of grid size and mesh quality on the results of numerical simulations. The agitated vessel is equipped with up-pumping pitched blade turbine (PBT). The computations were executed for a Newtonian liquid in turbulent flow. To model the

movement of the impeller, Multiple Reference Frame(MRF) or Sliding Mesh(SM) methods were applied. Geometrical measures of mesh quality were compared for each numerical grid. This study reported that the results of the numerical modeling of the flow field in the agitated vessel depend on the grid density and geometrical mesh quality.

Ameur et al.,2011 had studied non-Newtonian fluids. An agitated vessel equipped with a Scaba impellers is used. The CFD package (CFX 12.0) was used to solve the 3D hydrodynamics. The impact of agitator speed, location and blade size on the fluid flow and power consumption was examined. An increase in blade size is profitable for enlargement of the well stirred region, but power consumption is increased as a consequence of this. A short distance between the impeller and the tank walls restricts the flow around the agitator and yields higher power consumption. So, the absolute middle of the tank is appropriate position for this kind of impeller. The results obtained are compared with experimental data and a good agreement was found.

Babu,2010 had researched on the heat transfer coefficient in an cylindrical stirred vessel. The immiscible liquid systems at different operating conditions had been studied. The effect of heat transfer coefficient on speed of stirred, liquid properties, cooling water flow rate and location of agitator were analyzed. The empirical correlation was proposed for heat transfer coefficient in term of Nusselt number combines with Reynolds number, Prandtle number, volume ration and depth of turbine.

Driss et al.,2010 had studied the turbulent flow field in a stirred tank equipped with the pitched blade turbines (PBT). The three-dimensional flow is numerically studied using the Navier-Stokes equations in conjunction with standard k- turbulence model. The effects of inclined angle on local and global flow characteristics had been observed. The Computer simulations results for power numbers and flow patterns were measured and compared with previous literature.

Yoshida et al.,2009 had examined the progress of mixing of Newtonian liquid phase experimentally. The impeller power characteristics for an unbaffled agitated vessel with an angularly oscillating impeller were studied. The rotation of the impeller continues and periodically reversing its direction at a set angle. Results obtained from the angular oscillation mode of a disk turbine with six flat blades were compared at different amplitudes. The turbulent and laminar mixings were adequate, respectively, with higher and lower amplitudes. The mixing characteristics for turbulent and laminar flow regions were considered on the basis of the flow field features.

Ochieng et al.,2009 had reported that both the integrated experimental and CFD approaches had been employed to determine flow field. Both CFD and LDV data predicts the existence of flow misdistributions caused by the design of system. Consequently, the configurations may not provide the optimal operating conditions with reference to the system homogeneity and power consumption. The grid should be more refine to capture turbulent structures at microlevel. This would further amend the quality of the simulation results.

Deglon et al.,2006 had predicted that the Multiple Reference Frames (MRF) model and standard k- turbulence model can accurately model turbulent flow, if very fine grids coupled with higher-order discretization schemes are used. The MRF model give satisfactory results for the steady-state simulation but the k- turbulence model generally under or over-predicts turbulence. Simulations are conducted on four grids of considerably different resolution. The upwind, central and QUICK discretization schemes were used. The results were checked in terms of mean velocity components, power number and turbulent kinetic energy using previous literature. The general flow field and mean fluid velocity predictions were not strongly approached by either the grid resolution or discretization scheme, Whereas turbulent kinetic energy predictions are easily

approached by both the grid resolution and discretization scheme. This paper presents the poor predictions of turbulence obtained using the k- turbulence model.

Montante et al.,2006 had investigated the effect of the shaft eccentricity on the hydrodynamics of unbaffled agitated vessels. By comparing the experimental and simulated mean flow fields, it was found that the calculations based on Reynolds-averaged Navier–Stokes equations were applicable to get accurate results. The results obtained with the Reynolds stress model are admirable to that of the k- model.

Barbara et al.,2005 had studied the CFD modeling of the turbulent heat transfer in an agitated vessel. Four turbulence models, i.e. the standard k- and optimized Chen-Kim and also the standard k- and shear-stress transport models along with two near-wall region models were used in the modeling. The predicted local values of the heat transfer coefficient favorably compared with the experimental data from literature.

Kumaresan et al.,2005 had predicted that the flow pattern, mixing time, and power consumption in a stirred vessel depend on the impeller design, tank geometry and internal conditions. Measurements had been carried out in a stirred vessel for a standard 45° pitched-blade turbine and for a hydrofoil impeller. The comparison of the flow pattern had been given on the basis of equal power consumption to depict the extent of interaction between the rotating impeller and the internals.

Engeskaug et al.,2005 had studied the local wall heat-transfer coefficients for water and for the non-Newtonian liquids. The results were compared to existing correlations, and good agreement was observed for the water system outside the impeller region. For the non-Newtonian systems, a functional relationship between the Reynolds number and the heat-transfer coefficient was found to fit the data. Validation was done by a closer examination of the existing literature.

Barbara et al.,2004 had researched on the turbulent heat transfer for a stirred tank equipped with a Ruston turbine impeller and four standard baffles. Eight different types of turbulence models. In all investigated cases, the boundary flow at the vessel wall was given by the standard logarithmic wall functions. The values of the local heat transfer coefficient were compared with the corresponding experimental data. The best agreement was predicted for the standard $k-\epsilon$, optimized Chen-Kim $k-\epsilon$ and $k-\omega$ SST models.

Aubin et al.,2004 had reported the effect of the turbulence model, discretization scheme , modeling approach, turbulent kinetic energy and quantities such as the power and circulation numbers. The results have been validated with LDV data. The choice of stationary and time-dependent modeling approaches have little effect on the turbulent flow. Due to convergence difficulties faced with Reynolds Stress Model (RSM), the type of the turbulence model was restricted to the $k-\epsilon$ and RNG models. The mean flow and turbulent kinetic energy have little effect of these models and better agreement was predicted for the up-pumping pitched blade turbine. The power numbers were in good agreement for the down and up-pumping data.

Nere et al.,2003 had analyzed the liquid-phase mixing in a turbulent flow regime. The effects of the impeller design, the location of the impeller and the vessel size had been critically studied. The conclusions had been made for the selection of an energy-efficient impeller-vessel configuration.

Karcz et al.,2002 had studied the efficiency of the heat transfer process in a unbaffled, jacketed agitated vessel having eccentrically located impeller. The measured values of the heat transfer coefficient and power consumption was considered for the efficiency of the process. The measurements were carried out in the turbulent regimes.

Shekhar et al.,2002 had presented computations of the flow field, power consumption and mixing time. An agitated unbaffled vessel with eight-bladed paddle impeller was taken over a range of Reynolds numbers. The flow field calculations were carried out using the sliding mesh technique. The effect of grid size and the choice of the turbulence model were checked. The results showed satisfactory agreement by comparing with literature. It was observed in case of paddle impellers, that the product of mixing time and rotational speed remains unchanged for laminar flow.

Bakker et al.,2000 had examined the flow pattern for different Reynolds numbers. A pitched blade turbine was used. A sliding mesh method was used in the laminar regime. The impeller creates a radial flow pattern with low Reynolds number. The sliding mesh method is convincing for the prediction of flow patterns in stirred tanks. The results compared with experimental data obtained by Laser-Doppler-Velocimetry (LDV).

Armenante et al.,1999; had studied experimentally the power consumed by single, double, and triple down pumping, 45° six-bladed pitched-blade turbines (6-PBTs) under turbulent conditions. The turbines are located on the same shaft in stirred tank.. The total power consumption and power carried by each individual impeller (in single or multiple impeller configurations) was measured. The overall power numbers of double 6-PBT systems were typically detected to be smaller than twice the power number of a single 6-PBT. By Reducing the distance between the impellers the overall power number was lowered. Similar results were achieved with triple 6-PBTs.

Mavros et al.,1998 had used Laser Doppler velocimeter (LDV) measurements to calculate the turbulence structure for three agitators, namely a Rushton turbine and two axial agitators of different shape. Although the Mixel TT had the highest efficiency, but in a viscous liquid all

three had comparably low efficiency. Energy was dissipated mainly in circulation loop and in the stream flowing out of the impeller region. The mean and rms velocities were found to simulate stochastically the flow in agitated vessels.

Armenante et al.,1997 had studied the velocity profiles and turbulent kinetic energy distribution. An unbaffled, flat-bottom cylindrical tank equipped with a six blade, 45° Pitched blade turbine provided with a lid was investigated. The mean and fluctuating velocities in x, y and z directions were experimentally measured with Laser-Doppler Velocimeter (LDV) at five different heights and twenty radial positions within the cylinder. Fluent was used to numerically predict the velocity distribution, power consumption, fluctuating velocities and pumping capacity of the impeller. The k- model and algebraic stress model (ASM) was used to simulate the turbulence. Good agreement was found between numerical results and experimental data. Tangential velocities were bigger than the axial and radial velocities. The dimensionless mean velocities and dimensionless turbulent kinetic energy were found to be nearly independent of the impeller rotation speed.

Armenante et al.,1996 had studied experimentally and numerically the velocities in a baffled vessel having one or two 45° pitched-blade turbines by a Laser-Doppler Velocimeter (LDV) and a CFD software package (FLUENT) .The flow near impeller region was determined by LDV and used as boundary conditions in the numerical computations. Turbulence simulation were performed using either the k-ε model or Algebraic Stress Model (ASM). A comparison was made between CFD predictions and LDV measurements in terms of average velocities in all x, y, z directions as well as turbulent kinetic energies. Predictions based on ASM were in good agreement to the experimental data rather the k-ε model. Flow patterns in both configurations

were controlled by the axial and tangential components. The presence of the upper impeller amend the flow and produce a strong vertical recirculation pattern.

Sahu et al.,1995 had studied the standard k- turbulence model to numerically simulate the flow in an agitated baffled cylindrical tank with axial flow impellers. Three numerical schemes, i.e upwind scheme, hybrid scheme, and power-law scheme, has been used to decide the competitiveness of the various schemes. The solutions were caused by using the SIMPLE algorithm. The effects of initial assumed values of the flow variables, on the rate of convergence were analyzed. The sensitivity of the model parameters on the flow characteristics, the effects of global grid sizes and near-wall grid sizes was checked thoroughly. The boundary conditions in the impeller region for the velocities and turbulent kinetic energy were taken from the experimental data. Computations were carried out using six different impeller designs and was found that the predicted values were qualitatively good with the experimental data.

Kumpinsky.,1995 had studied the thermal performance of stirred vessels with coils and jackets. Performance is carried out with the computation of heat-transfer coefficients by offering heating and cooling data into model equations. Two model categories i.e., differential and macroscopic were studied, the latter is adopted due to mathematical simplicity and lower sensitivity to experimental data variability.

Haam et al.,1993 had predicted the process-side heat-transfer coefficients followed by mixing with a high-efficiency impeller. Each impeller (of different diameters) was evaluated to consider its effects on the mixing parameters of the tank. To obtain a range of Reynolds numbers Impeller speed was varied. The exponents for the normally judged empirical heat-transfer equation were analyzed for each component.

Askew et al., 1965 had studied the local heat transfer coefficients at the wall of a baffled cylindrical vessel having flat-bottom & centrally agitated. The local heat transfer coefficients was given as functions of vertical and radial position for 90° turbine, 45° turbine. The Impeller size, speed, and clearance were considered as variables. The results were predicted in terms of Nusselt, Reynolds and Prandtl number correlations for a Reynolds number ranging from 200 to 175,000 and a Prandtl number ranging from 5 to 2000. The local heat transfer coefficient was act a function of the power input to the system generated by the impeller.

CHAPTER-03

PROBLEM STATEMENT AND MATHEMATICAL MODELLING

This chapter presents description of the problem statement, geometrical configurations of the agitated vessel and the mathematical equations governing the flow and heat transfer in an agitated vessel together with relative boundary conditions.

3.1 Problem Statement

In the present work, CFD Simulation of three dimensional turbulent heat transfer for a single phase Newtonian liquid under steady state condition in an unbaffled, jacked agitated vessel equipped with a down-pumping Pitched Blade Turbine (PBT) having Six blades at 45° , have been performed using ANSYS Fluent.

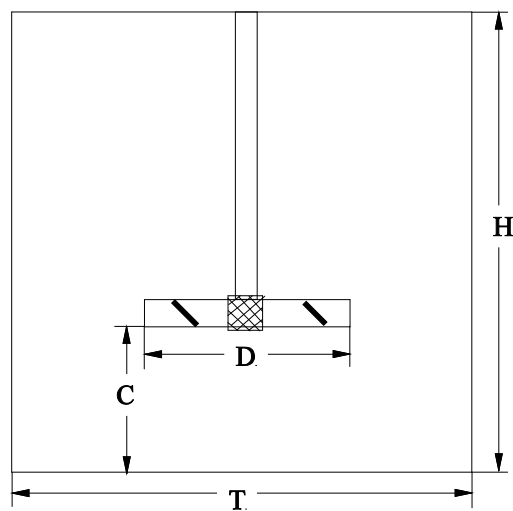


Figure 3.1 Schematic diagram of the investigated agitated vessel.

3.2 Geometrical configuration

The system under investigation in the present work is the flat-bottom, unbaffled cylindrical agitated vessel equipped with a six-blade 45° Pitched blade turbine (PBT). The tank is filled with water upto the level $H=T$. A schematic diagram of the agitated vessel is depicted in figure 3.1. The tank geometry and fluid properties are similar to the properties taken by Armenante et al.,1997. Agitation is provided by the impeller mounted on a concentric shaft inside the cylindrical tank. The impeller have 0.073m off-bottom clearance from the tank bottom. The dimensional data for the agitated vessel and impeller is shown in table 3.1 and the fluid properties and numerical parameters are listed in table 3.2.

Table 3.1 Dimensional data of the Agitated Vessel

Item	Symbol	Dimension
Vessel diameter	T	0.293m
Vessel height / liquid height	H	0.293m
Impeller diameter	$D=T/3$	0.097m
Width of impeller blade	w	0.0196m
Off –bottom clearance	$C=T/4$	0.073m
Blade thickness	t	2mm
No. o blades	n	6

Table 3.2 Fluid properties and other important parameters

Item	Symbol	Value
Density		$1 \times 10^3 \text{ Kg.m}^{-3}$
Dynamic viscosity	μ	$1 \times 10^{-3} \text{ Pa.s}$
Impeller Speed	N	7.5 s^{-1}
Blade tip speed	U_{tip}	2.3 m.s^{-1}
Reynolds Number	$Re = ND^2/\mu$	7.2×10^4

3.3 Governing Differential Equations

The governing equations for three dimensional fluid flow are the continuity, the x-, y- and z components of momentum equation and the thermal energy equation written as below. The governing equations are given in cartesian co-ordinate system. The components of velocity in x-, y- and z- direction are u, v, and w respectively.

Equation of Continuity

$$\left(\frac{\partial}{\partial t} + \frac{\partial(\rho u)}{\partial x} + \frac{\partial(\rho v)}{\partial y} + \frac{\partial(\rho w)}{\partial z} \right) = 0 \quad (1)$$

Where ρ is the density and for incompressible fluids $\rho = \text{constant}$.

x-Momentum equation

$$\rho \left(\frac{\partial u}{\partial t} + u \frac{\partial u}{\partial x} + v \frac{\partial u}{\partial y} + w \frac{\partial u}{\partial z} \right) = -\frac{\partial p}{\partial x} + \mu \left(\frac{\partial^2 u}{\partial x^2} + \frac{\partial^2 u}{\partial y^2} + \frac{\partial^2 u}{\partial z^2} \right) \quad (2)$$

y-Momentum equation

$$\rho \left(\frac{\partial v}{\partial t} + u \frac{\partial v}{\partial x} + v \frac{\partial v}{\partial y} + w \frac{\partial v}{\partial z} \right) = -\frac{\partial p}{\partial y} + \mu \left(\frac{\partial^2 v}{\partial x^2} + \frac{\partial^2 v}{\partial y^2} + \frac{\partial^2 v}{\partial z^2} \right) \quad (3)$$

z-Momentum equation

$$\rho \left(\frac{\partial w}{\partial t} + u \frac{\partial w}{\partial x} + v \frac{\partial w}{\partial y} + w \frac{\partial w}{\partial z} \right) = -\frac{\partial p}{\partial z} + \mu \left(\frac{\partial^2 w}{\partial x^2} + \frac{\partial^2 w}{\partial y^2} + \frac{\partial^2 w}{\partial z^2} \right) \quad (4)$$

Energy Equation

$$\rho_p \left(u \frac{\partial}{\partial x} + v \frac{\partial}{\partial y} + w \frac{\partial}{\partial z} \right) = k \left(\frac{\partial^2 T}{\partial x^2} + \frac{\partial^2 T}{\partial y^2} + \frac{\partial^2 T}{\partial z^2} \right) \quad (5)$$

3.4 Boundary Conditions

Top, Bottom & Walls of the vessel: There is no-slip condition applied on the vessel walls, so velocity is null. i.e $u = 0, v = 0$ and $w = 0$

Impeller: On all rigid walls, a setting of no-slip condition has been prescribed.

3.5 Some Dimensionless Groups

Dimensionless groups are commonly used in the mixing literature to correlate data in terms of physical properties, scalar quantities and time. Some dimensionless groups which are used in the present work, described in the following sub-sections.

3.5.1 Reynolds Number, (Re)

The Reynolds number is a group used to characterize the type of flow i.e. whether the flow is laminar or turbulent flow. It is the ratio of inertial forces to viscous forces. For an agitator the Reynolds number is defined as:

$$R = \frac{\rho D^2}{\mu} \quad (6)$$

3.5.2 Prandtl Number,(Pr)

It provides a measure of relative effectiveness of momentum and energy transfer. It is defined as the ratio of momentum diffusivity to the thermal diffusivity and mathematically defined as:

$$Pr = \frac{\mu C_p}{k} \quad (7)$$

3.5.3 Nusselt Number,(Nu)

It is the ratio of convective heat flux to conduction heat flux. Larger the value of Nusselt number indicates large convection in the fluid. Nu number is represented mathematically as:

$$N = \frac{hD}{k} \quad (8)$$

NUMERICAL METHODOLOGY

To predict the flow pattern and heat transfer, numerical approaches has been used. A computational fluid dynamics package ANSYS Fluent is used to solve the governing equations. The turbulent motion and heat transfer equations and associated turbulence models are introduced in this chapter to understand the methodology of turbulent flow and heat transfer simulations.

4.1 A Brief Introduction to CFD

The computational fluid dynamics (CFD) method has become a useful and powerful tool for solving fluid flow and heat transfer problems. The CFD uses numerical methods to solve the equations describing the conservation of mass, momentum and heat, together with some approximations. The main advantage of CFD simulation lies in its potential for reducing the extent and number of experiments required in industries. Modeling a stirred tank using CFD requires consideration of many aspects of the process. The motion of the impeller in the tank must be treated in a special way. The basic principle is to split the domain under investigation into small elements and for each elements, a set of partial differential equations is solved, which approximates a solution for the flow in order to achieve the conditions of conservation of mass and momentum. The basic equations are solved simultaneously with any additional equations implemented in a particular model to obtain the flow patterns, pressure, characteristics of turbulence and any derived quantities .

For easy access, CFD contains three main elements:

- Pre-processor
- Processor and
- Post-processor.

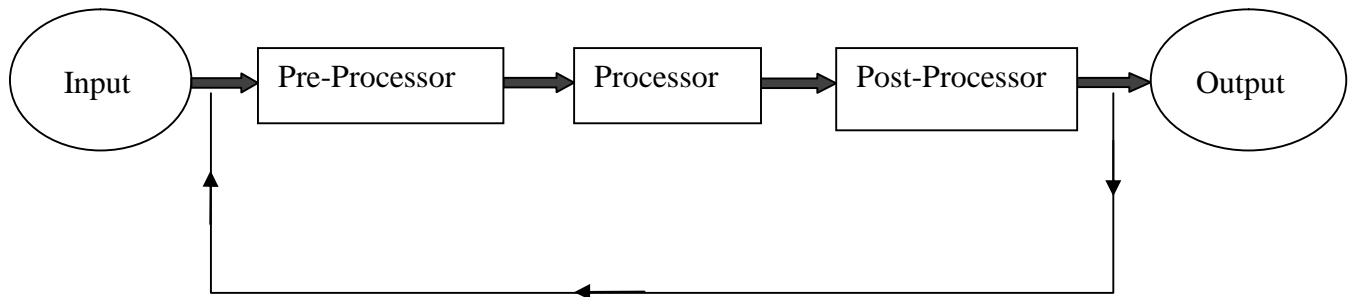


Fig. 4.1 Schematic presentation of CFD

4.1.1 Pre-processor

It serves as a source of input by means of an operator. The user's activities at the pre-processor stage involve the definition of geometry, mesh generation and specifications of the appropriate boundary conditions. The computational model requires that the volume occupied by the fluid, within the vessel to be described by a computational grids. In these grids, variables are computed and stored.

4.1.2 Processor

At this stage the solution of the Navier-stokes equations in conjunction with suitable model are developed by using a control volume discretization method. Numerical methods consist on an approximation of the unknown flow variables by means of simple functions and a discretization by substitution of the approximation into the governing flow equations and subsequent mathematical manipulations.

4.1.3 Post-processor

The great resources has been devoted for the development of post-processing techniques and display. These include geometry part, grid display, vector plots, surface plots and view manipulation. Several results can be obtained such as the velocity field, the viscous dissipation rate, the characteristics of turbulence etc. Also, it is possible to exchange data through the postprocessor with other interfaces

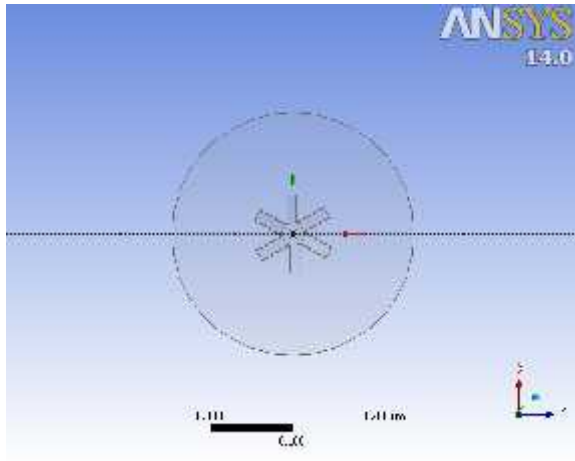
4.2 Numerical Methodology

For the unbaffled, concentrically agitated vessel, the boundaries of both the rotating impeller and the stationary vessel walls are axisymmetric to the rotating axis, so that the fluid flow problem can be solved simply by using a single reference frame moving with the impeller. In this rotating frame, the impeller speed is zero and the tank wall is assigned a rotational speed opposite that of the reference frame. Double precision was used for the simulations in this work. The convergence can be improved by running the simulation in double precision. No-slip boundary conditions are applied to the tank walls, bottom, shaft, and the impeller. The liquid surface is assumed as a flat surface and is modeled using a y-symmetry condition. The Three dimensional steady flow of water inside a 0.293m diameter tank agitated by a 45° six-blade impeller with 0.073m clearance was simulated using CFD package ANSYS FLUENT 14.0. The finite volume method is implemented in this solver. The computational domain, adopted from Armenante et al., 1997, was discretized into number of cells. In this way, governing equations are solved in a rotating reference frame to handle the impeller rotation, while in the rest of the vessel the flow is calculated by solving the RANS equations in a stationary reference frame. The combination of continuity and momentum equations were solved using a Semi-Implicit Method for Pressure-

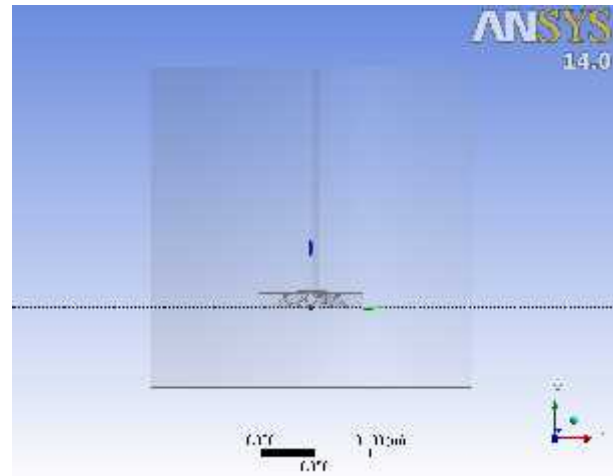
Linked Equations (SIMPLE) algorithm and a second upwind discretization scheme. The SIMPLE algorithm coupled the continuity and momentum equations to derive the pressure field inside the tank, and the momentum discretization was computed by a second-order upwind method. The transport equations are integrated over its own control volume using hybrid scheme. In this study, the impeller speed was 7.5s^{-1} . The vessel was simulated using periodic boundary conditions. A standard scheme was used to compute the pressure part. The velocity fields obtained by solving the Navier-Stokes equations are used as the input to the energy equation. The explicit scheme is used for the solution of energy equation to obtain the temperature field. The solution is considered to be fully converged when the normalized residuals of all variables fell below 10^{-6} .

4.3 Simulated Geometry

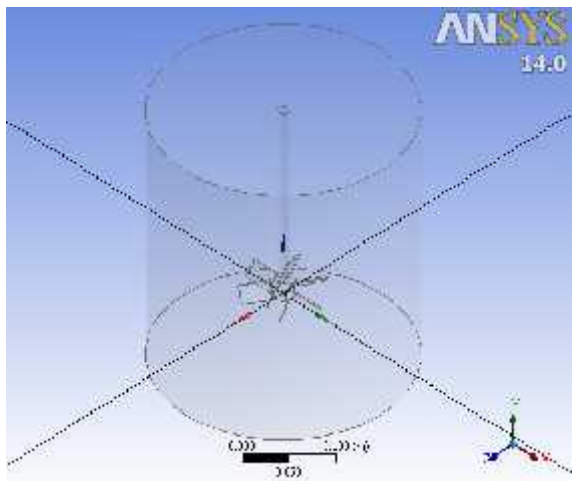
The agitated vessel and impeller are modeled with the same geometry as used by Armenante et al., 1997, using the WORKBENCH 14.0 Platform. The simulations are performed with water as a liquid, filled upto the top so that vortex formation is eliminated in the vessel. As we used the WORKBENCH 14.0 platform, all the graphics and snapshots are presented in cartesian coordinates: x and z axes are located in the horizontal plane and y-axis is vertical as shown in figure 4.2.



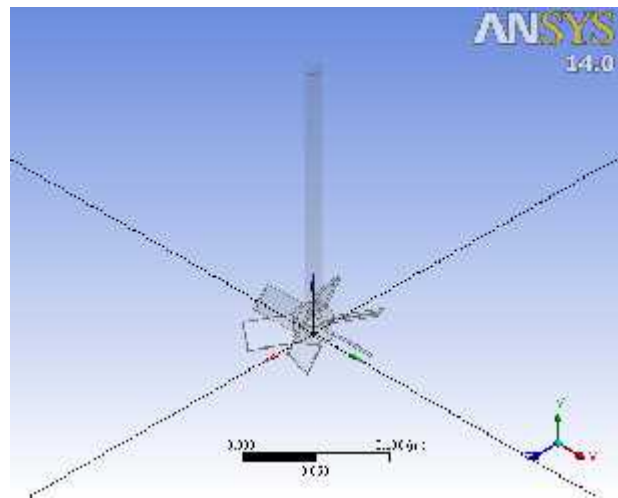
(a)



(b)



(c)



(d)

Figure. 4.2 Simulated geometry of agitated vessel and Impeller: (a) Top view, (b) Front view, (c) Isometric view, (d) Isometric view of Impeller.

4.4 Rotating Coordinate System

A rotating coordinate system can be set up in Fluent 14.0. In such a system the reference frame of the body rotates with a constant angular velocity about a fixed axis. For the particular calculation in a unbaffled tank, a rotating reference frame may be used to avoid the need for complicated impeller boundary conditions. In this reference frame the tank is rotating at the same angular velocity (), but in the opposite direction, and the impeller is stationary, creating blockage to the flow. This corresponds to taking a body of fluid and rotating its boundaries at a constant angular velocity (). Then at any time after starting the rotation, the whole body is rotating with this same angular velocity and moving as if it was a rigid body. Then there are no viscous stresses acting within the fluid, and the velocity field is given by:

$$\mathbf{u} = \boldsymbol{\omega} \times \mathbf{r} \quad (9)$$

\mathbf{u} is the velocity vector and \mathbf{r} is distance tensor. The disturbance produced by impeller would produce a motion in a non-rotating system, that will produce a motion relative to this rigid body rotation. This motion can be considered as the flow pattern, and is defined as the pattern that will be observed by an observer fixed to the rotating boundaries.

4.5 Grid Generation

To solve Navier-Stokes equations in the required flow domain, one need to divide the flow domain into a number of square or rectangular region of equal or unequal size known as cells. The type of grid/mesh depends upon location of scalars and vectors in the domain. For example, if all the scalar (e.g., pressure, viscosity and temperature, etc.) and vectors (e.g., velocity) are defined at the centre of the cell, it is known as normal or collocated grid. While if scalars are defined at the centre of the cells and vectors are defined at the centre of the cell faces on which

they are normal, then it is known as staggered grid (Zhang, 1998). The resolution of the computational grid is a key factor in any CFD simulation, as this is directly related to the computational cost of the solution. Grids reported in the various studies of stirred tanks range from an order of about 10^4 to about 10^6 control volumes for the simulation of agitated vessels of similar dimensions. To determine the grid resolution required to get a solution, it is necessary to perform simulations on successively refined grids until no notable difference in the predicted values of the important solution variables are observed. The grid sensitivity test is performed on successively refined grids from about 10^4 to 4×10^5 control volumes and It is predicted that the successively finer grids yielded equivalent predictions of mean velocity profiles which were in good agreement with experimental LDV data. Therefore the fine grids give results in better agreement than do the coarser grids. A tetrahedrons meshing is applied on the system geometry. The computational mesh of our system geometry contains 86924 nodes. The generated mesh on the impeller and Agitated vessel in different planes are shown in figure 4.4.

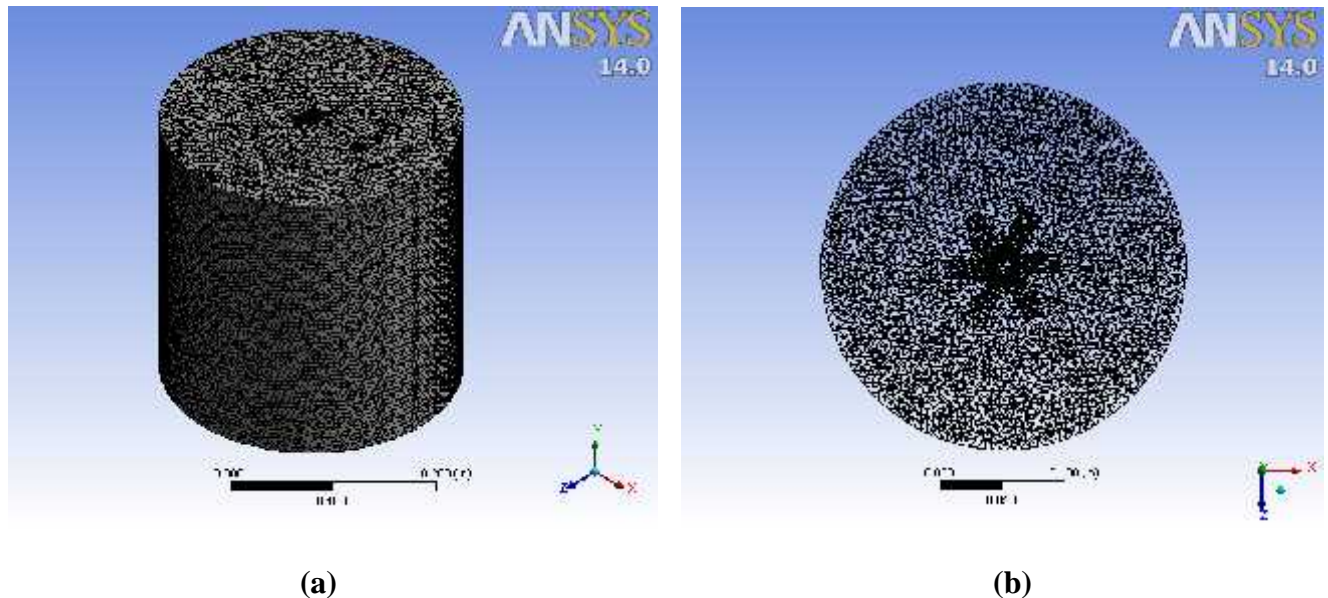


Figure.4.3 Grid for Impeller and vessel:

(a) Front View(shaded view), (b) Top view (wire frame)

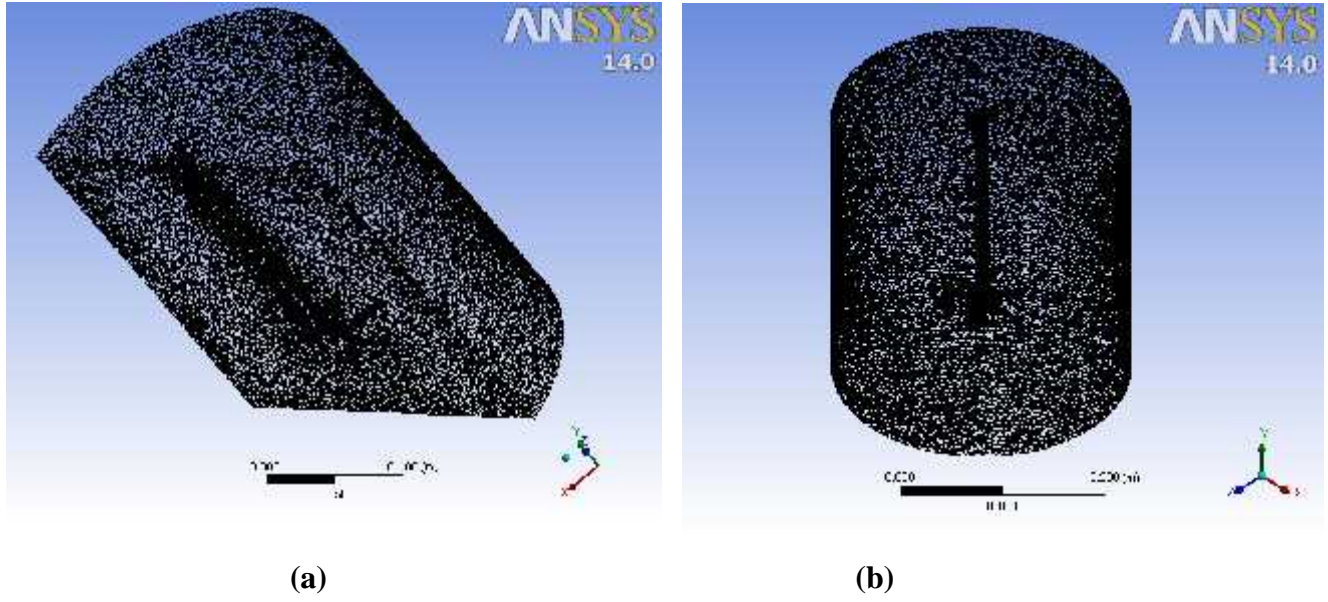


Figure 4.4 Grid for Impeller and vessel in wire frame:

(a) Cut-sections view, (b) Isometric view

4.6 Turbulence model

Turbulence consists of fluctuation and randomness in the flow field with time and space. It is a complex process, mainly because it is three dimensional, unsteady and consist of many levels. It affects the heavily flow. Turbulence generally occurs when the inertia forces in the field becomes significant compared to viscous forces, and is characterized be a high Reynolds number. In principle, the Navier-stockes equations describe both laminar and turbulent flows without the need for additional information. Turbulence model are used to predict the effect of turbulence in fluid flow without resolving all scales of the smallest turbulence fluctuations. Many models have been developed that can be used to approximate turbulence based on the Reynolds Average Navier-Stocks equations. Some models have very specific applications while other can be applied to a wider class of flow with a reasonable degree of mixing. One of the main problem in turbulence modeling is the accurate prediction of flow separation from a smooth surface.

Standard two equation turbulence models often fail to predict the onset and the amount of flow separation under high pressure gradient conditions. In general, turbulence model based on two equation predicts the onset of separation too late and under-predict the amount of separation later on. This behavior gives an overly optimistic performance characteristic of the system. However, we generally used two equation models because of their simplicity and lesser computational time. Since the Reynolds-averaged equations cannot be solved directly therefore certain simplifications should be made to close the equations from a mathematical standpoint. The different simplified methods used for the fluctuations produced, results in different types of turbulence models. The turbulence models can be classified as one-equation models and two-equation models. In general, one-equation models employs the transport equation of turbulent kinetic energy only, and two-equation models account for the transport of turbulent kinetic energy dissipation rate. In this work only two-equation models, are considered. For this particular research, the standard k- model and other related models are introduced here.

4.6.1 Standard k- Turbulence Model

It is one of the most prominent turbulence model and has been applied in most general purposes. It is considered as the industry standard model. This model is stable and numerically robust. For general purpose simulation, the model offers a good agreement in term of accuracy and robustness (Mitesh, 2013) .The k- turbulence model uses the scalable wall functions approach to improve robustness and accuracy near wall meshes. The k- turbulence model provides good predictions for many flows. Here, k is the turbulence kinetic energy and is defined as the Variance of the fluctuations in velocity. It has dimensions of m^2s^{-2} .The (epsilon) is the turbulence eddy dissipation i.e the rate at which the velocity fluctuations dissipate.

4.6.2 k- Turbulence Model

One of the merit of k- Turbulence Model is near wall treatment for low Reynolds number computations. This Model does not involve the complex non-linear damping functions and is therefore more accurate and more robust. The model assumes that the turbulence viscosity is linked to the turbulence kinetic energy and turbulent frequency.

4.6.3 Shear Stress Transport Model

The shear stress transport model was designed to give highly accurate predictions of flow and the amount of the flow separation under adverse pressure gradients by the inclusion of transport effect which results in a major improvement in terms of flow separation. The SST model is recommended for high accuracy boundary layer simulations

CHAPTER-05

RESULT AND DISCUSSION

This chapter presents the results obtained from the study of three dimensional unbaffled agitated vessel. The velocity profiles and temperature profiles three different locations. The results obtained are compared with experimental data.

5.1 Validation of the Present work

The numerically predicted velocity and experimental LDV velocity from (Armenante et al.,1997) are compared at axial height $Y=88\text{mm}$ shown in figure 5.4. The results for the axial, radial and tangential components of velocity are normalized by the impeller blade tip velocity at this axial height $Y=88$ are shown in figure 5.1,5.2 and 5.3.

5.1.1 Axial Velocity comparison

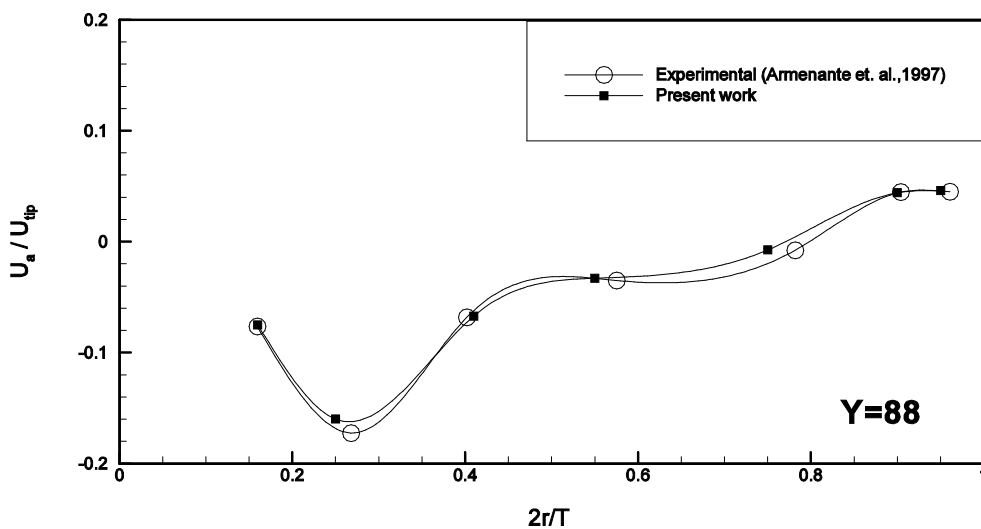


Figure 5.1 Axial velocity at horizontal location $y = 88$

The figure 5.1 shows a very good agreement between the experimental and numerical results predicted for the axial velocity. The simulation typically overpredicted the experimentally obtained velocities near the bottom of the vessel. It is reported that the reproducibility of the Experimental LDV velocity in the region below the impeller was not as good as in the rest of the vessel. The reason behind this, is the lower values of the velocities and the fluctuation of the secondary flow pattern which is observed just below the pitched blade turbine.

5.1.2 Radial Velocity Comparison

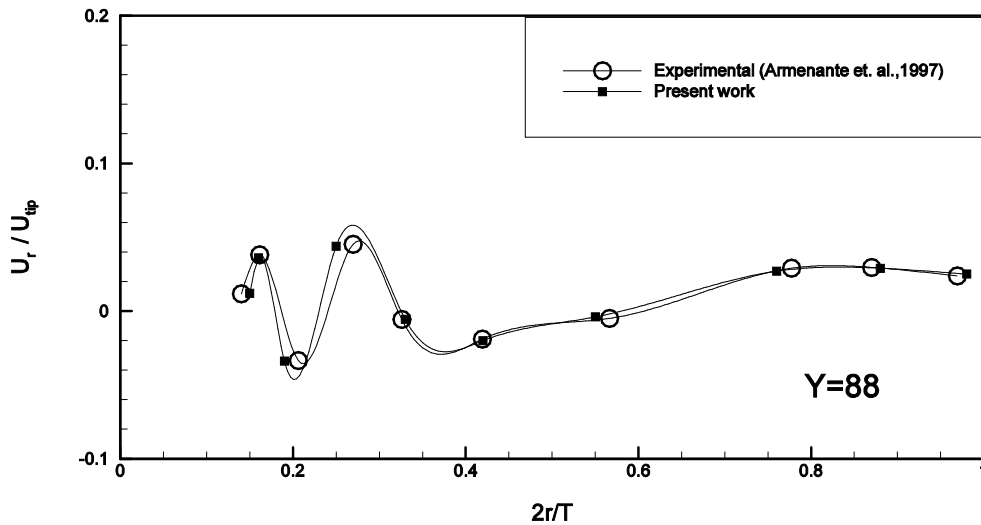


Figure 5.2 Radial velocity at horizontal location $y = 88$

The corresponding data of radial velocity are presented in the figure 5.2. The radial velocities points are a little bit inward above the impeller but well-founded outward on the lower side of the impeller. The experimental and numerical velocities above the impeller are predicted satisfactorily.

5.1.3 Tangential Velocity Comparison

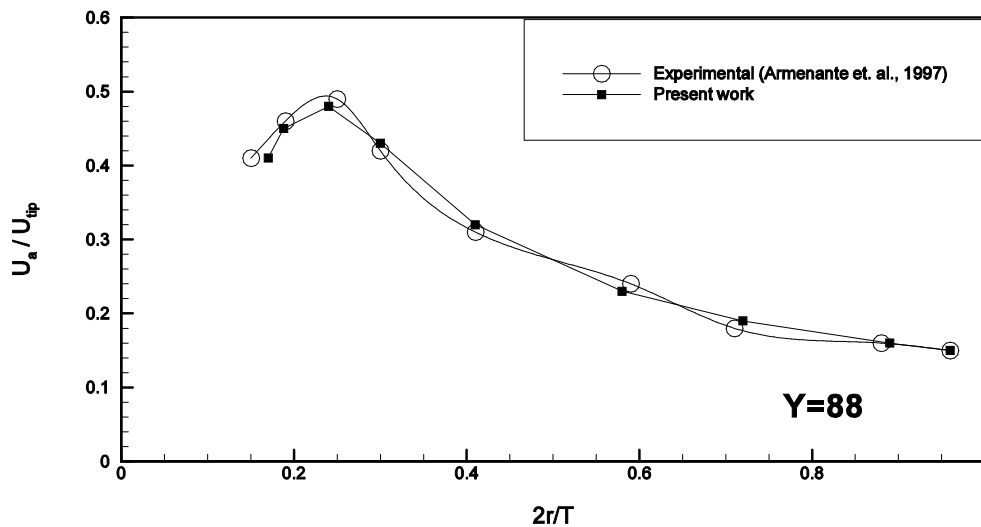


Figure 5.3 Tangential velocity at horizontal location $y = 88$

The tangential velocities obtained by experimental and numerical method in the vicinity of the impeller are shown in figure 5.3. The tangential velocity profile near the tip of the impeller is maximum but towards the wall of the vessel it is decreasing.

5.2 Flow Field Analysis

5.2.1 Velocity

The predicted mean flow pattern in terms of velocity in different plane at different locations in a agitated vessel equipped with pitched blade turbine is to be discussed here. The predictions were obtained corresponding to $Re = 7.2 \times 10^4$. The axial velocities above and below the impeller are found to be all negative, as it was expected for a downward pumping impeller (Armenante et al., 1997). The velocities above the impeller are quite low and uniform, whereas those below the impeller shows a strong downward pumping action near the outer edge of the impeller.

The tangential velocities are maximum near the tip of the impeller. This pattern is consistent for a system similar to Armenante et al.,1994 , Nagata ,1975 and Dong et al.,1994a,b. The location of different plane considered in this study are shown in figure 5.4. The top plane is at $y = 160\text{mm}$, middle plane is $y = 82\text{mm}$ and bottom plane is at $y = 71\text{mm}$ from the bottom of the vessel in axial direction.

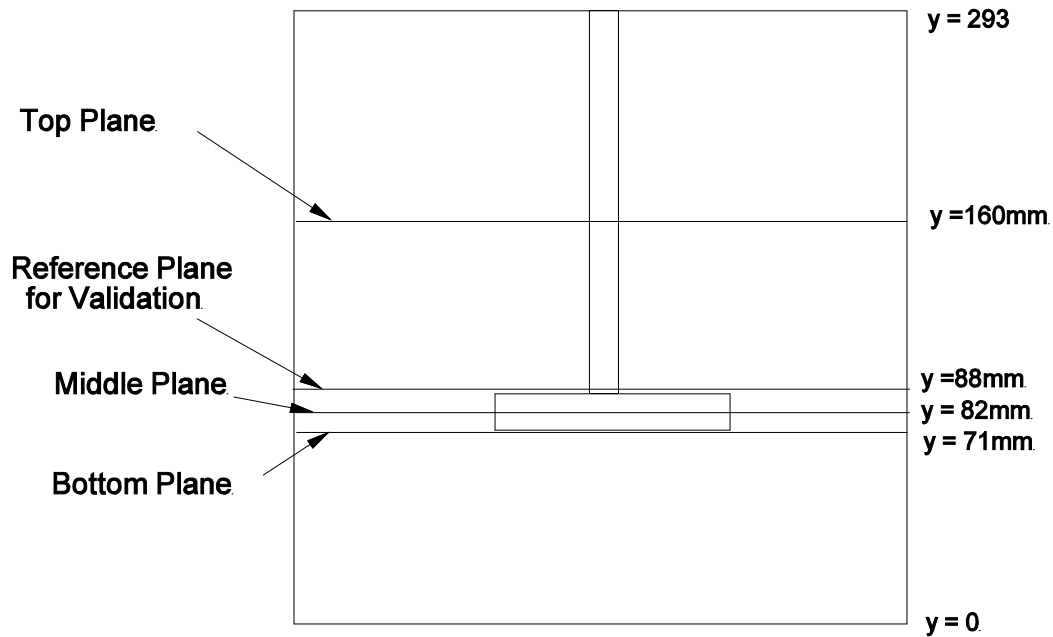
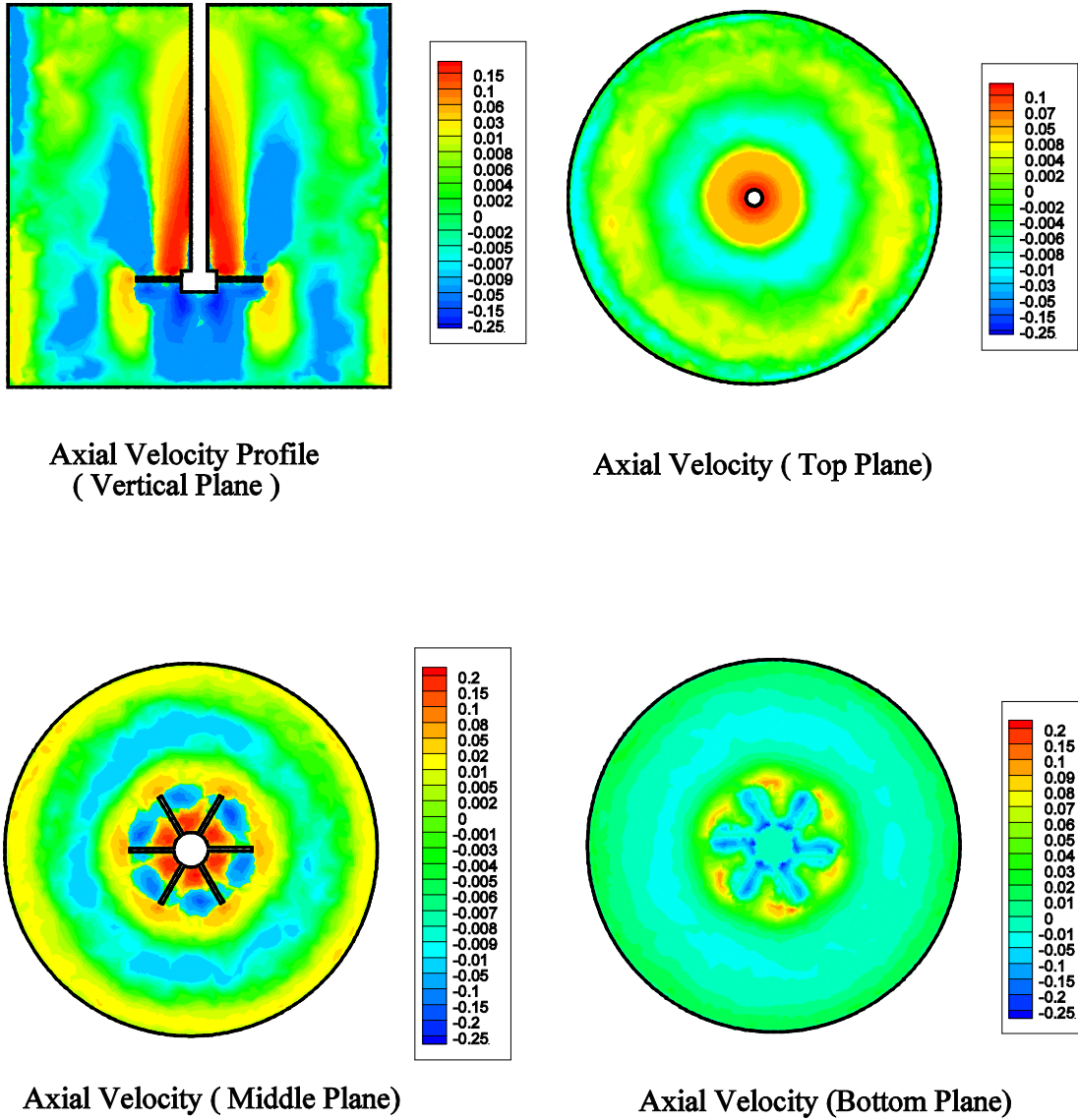


Figure 5.4 Location of different planes.

In the region just above the impeller, the flow in the z - y plane is mainly directed straight downward and feeding the impeller. In cylindrical region adjacent to the shaft, the numerically obtained velocity vectors are found to be very small. The main lower circulation flow in the region below the impeller is almost completely cut off. The velocity contours in axial, radial and tangential direction produced by the impeller are shown in figure 5.5, 5.6 and 5.7 respectively. As we are rotating the vessel instead off the impeller, so the results obtained for velocity are reversed in manner.

5.2.1(a) Axial Velocity contours



Axial Velocity Profile
(Vertical Plane)

Axial Velocity (Top Plane)

Axial Velocity (Middle Plane)

Axial Velocity (Bottom Plane)

Figure 5.5 Axial velocity contour at different cross-section of the vessel.

The axial velocity contours are shown in figure 5.5. It is predicted that there exist circulation loops below the impeller and the axial velocity in this region shows a strong downward pumping action of the impeller as shown by vertical plane. The axial velocity in middle plane shows that

velocity is higher in the impeller region. The axial velocities are lower in the region above the impeller as shown in top plane.

5.2.1(b) Radial Velocity contour

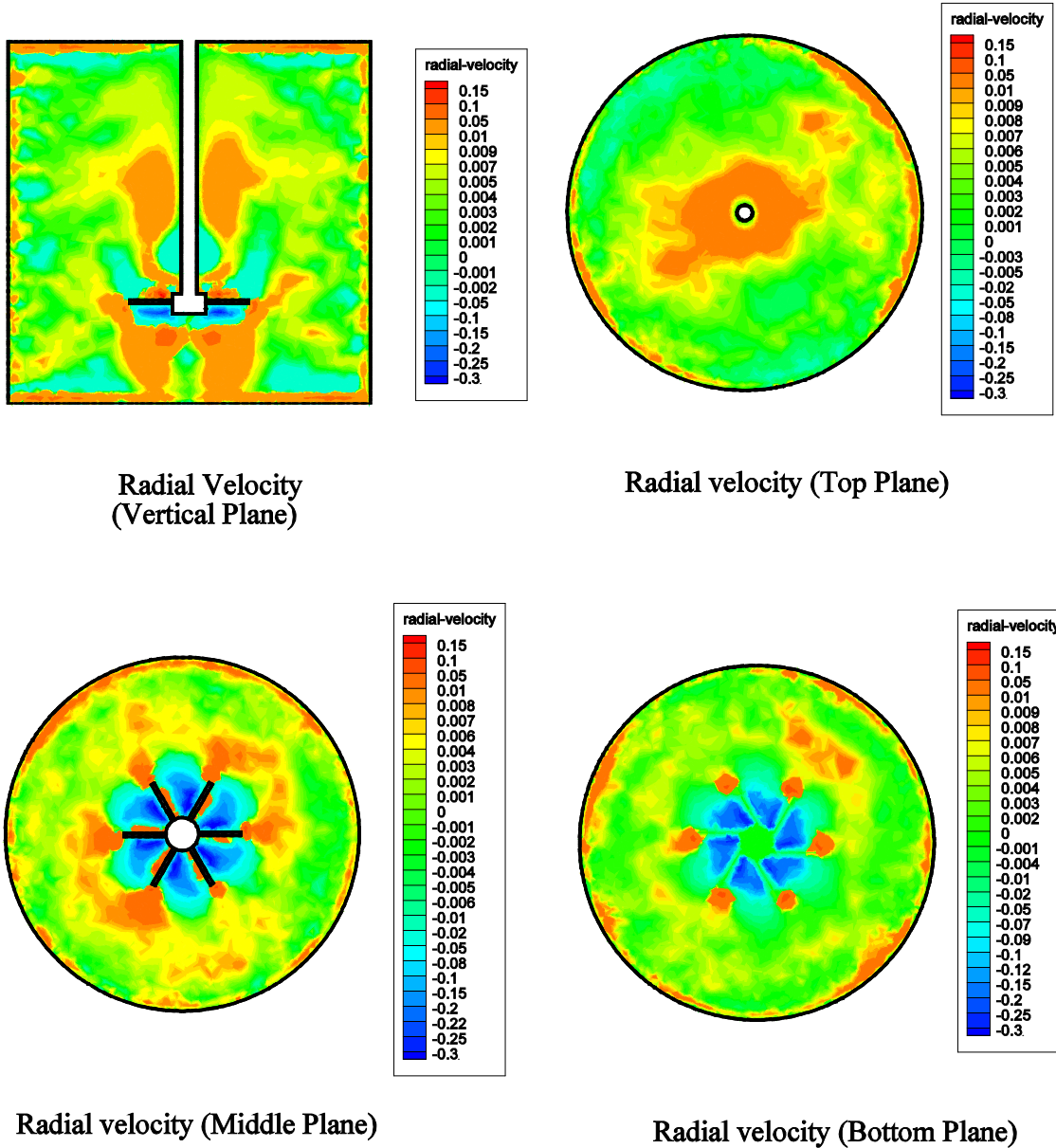


Fig.5.6 Radial velocity contour at different cross-section of the vessel.

It is predicted from figure 5.6 that the radial velocity is slightly inward above the impeller and strongly outward below the impeller as shown in vertical plane. The velocity below the impeller is low and high above the impeller.

5.2.1 (c) Tangential Velocity Contour

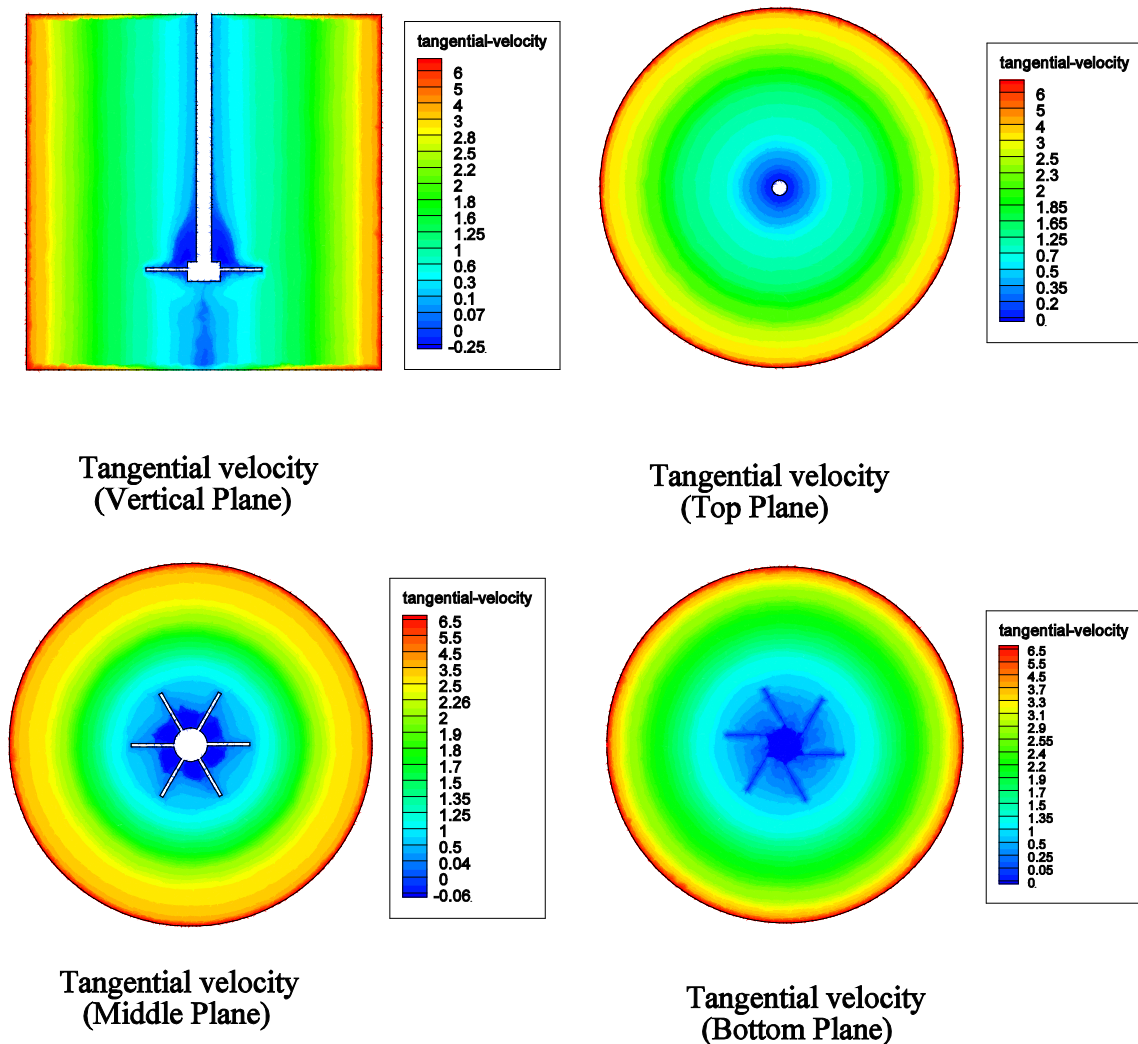


Figure 5.7 Tangential velocity contour at different cross-section of the vessel

From the tangential velocity contour as shown in figure 5.7, the Tangential velocity is maximum at the tip of the impeller and is minimum at the walls of the vessel.

5.2.2 Pressure

The effect of agitation on pressure inside the vessel is shown in figure 5.8. The pressure variation above the impeller, below the impeller and at middle of the impeller are shown. It is clear from these contour that the pressure is maximum at the walls of the vessel as the velocity is minimum in this region and it has minimum value in the impeller region because velocity is maximum here.

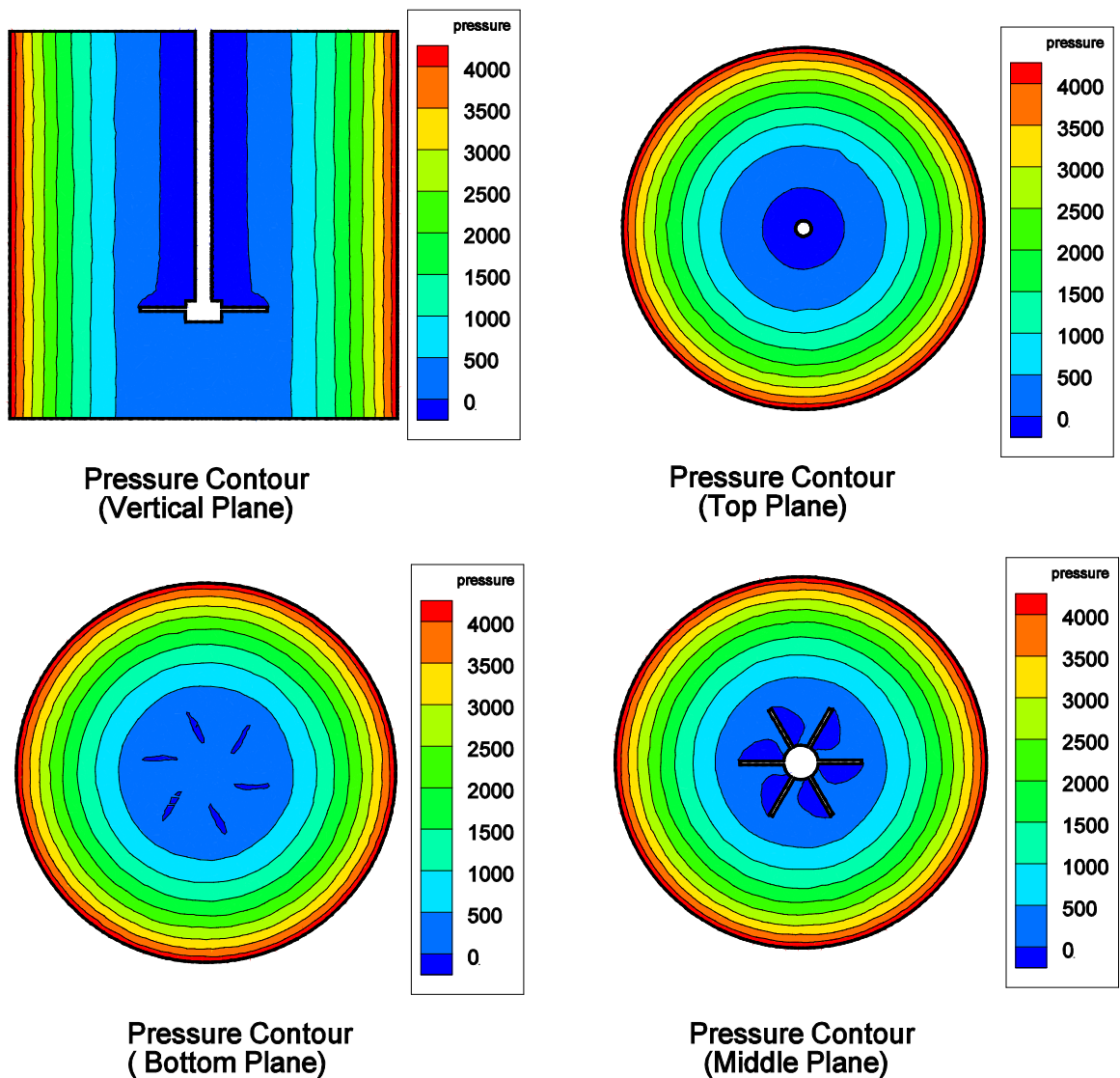


Figure 5.8 Pressure contours at different cross-section

5.3 Heat transfer

The heat transfer or distribution of temperature inside the jacketed vessel due to constant heat at different Prandtl number are shown in figure 5.9,5.10,5.11,5.12,5.13,5.14. Heat transfer is studied at $Re=7 \times 10^4$ by changing the Prandtl number(Pr). The simulations were done assuming steady state operation.

5.3.1 Isotherm

The temperature profile for $Pr=0.71$ is shown in figure 5.9 both in vertical and middle plane. It is observed that the temperature in the region near the impeller is lower and almost uniform whereas toward the outer wall region temperature is high. Here the temperature gradient has lower magnitude.

By increasing the Prandtl Number further i.e. 7, 20,30,40 and 50 respectively, the temperature gradient is further reduced and uniform temperature profile is obtained at $Pr = 50$.

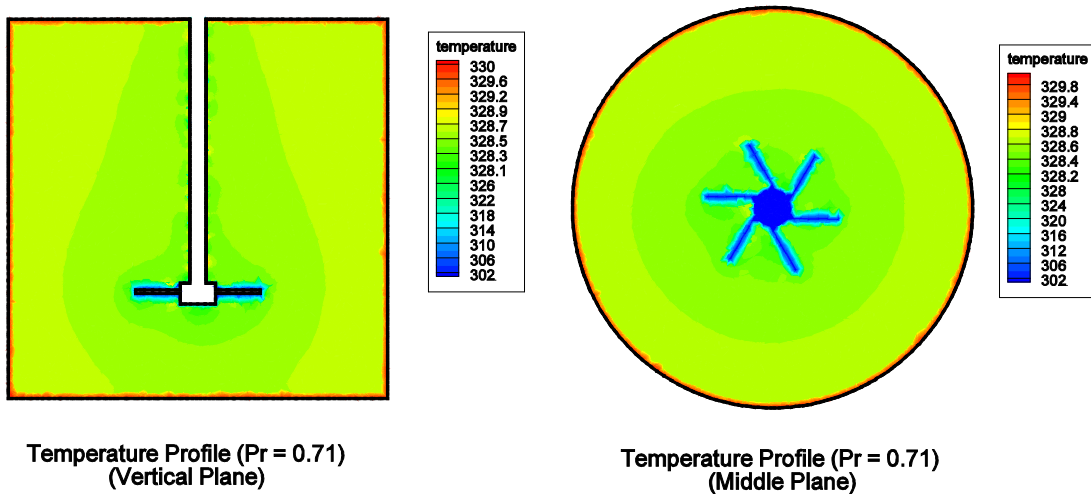
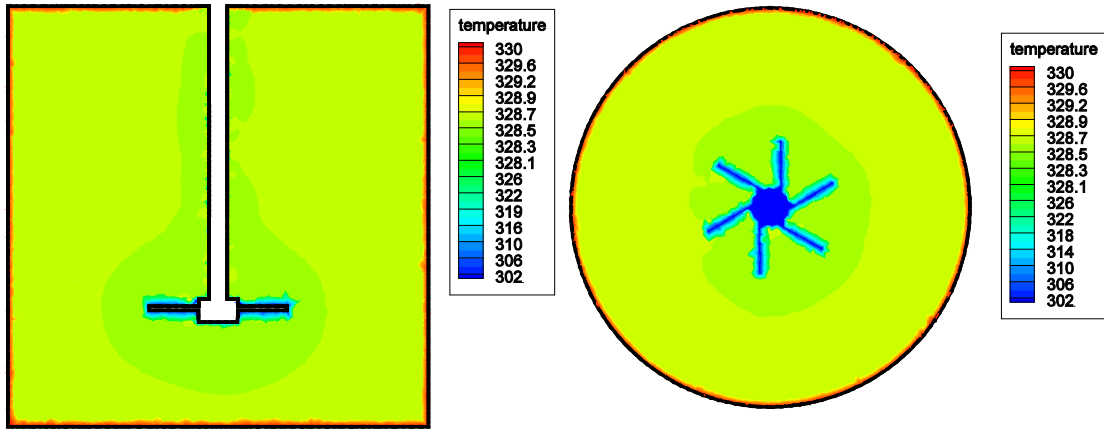


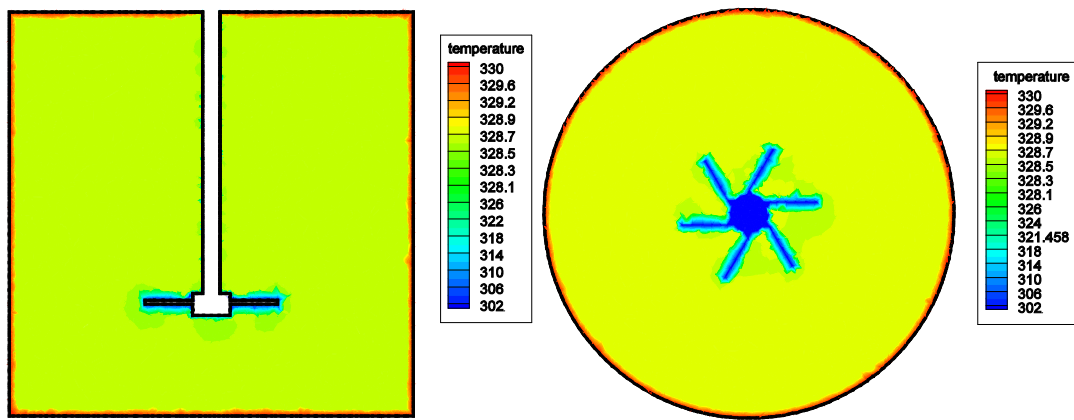
Figure 5.9 Temperature Profile for $Pr = 0.71$



Temperature Profile (Pr = 7)
(Vertical Plane)

Temperature Profile (Pr = 7)
(Middle Plane)

Figure 5.10 Temperature Profile for Pr =07



Temperature Profile (Pr = 20)
(Vertical Plane)

Temperature Profile (Pr = 20)
(Middle Plane)

Figure 5.11 Temperature Profile for Pr =20

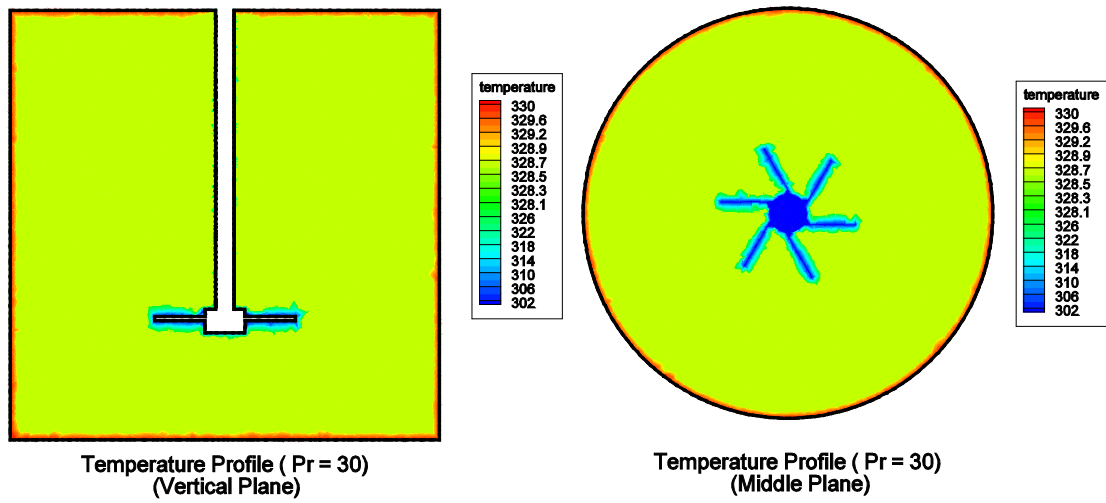


Figure 5.12 Temperature Profile for Pr =30

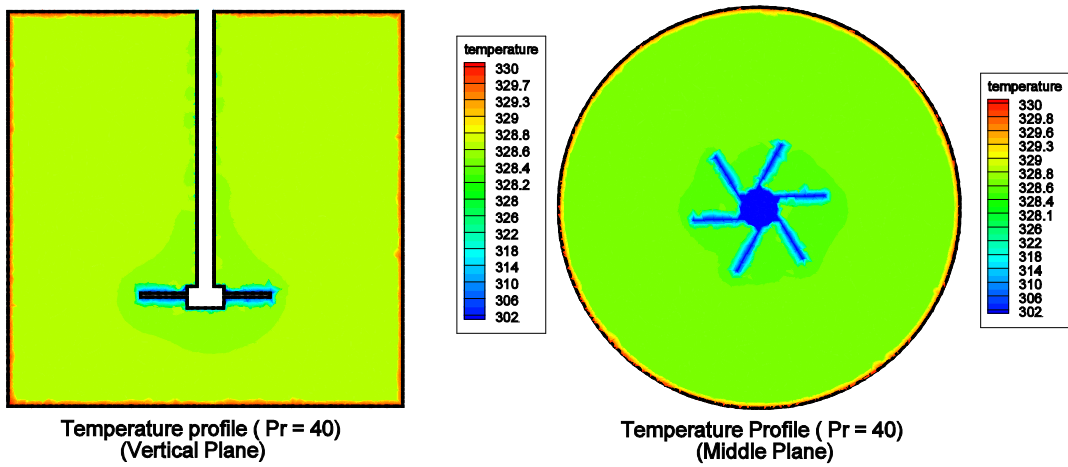


Figure 5.13 Temperature Profile for Pr =40

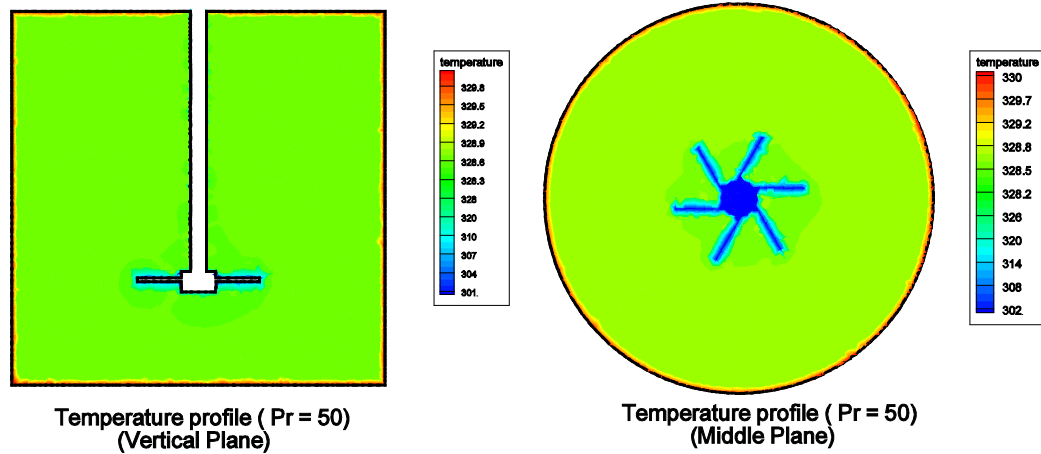


Figure 5.14 Temperature Profile for Pr =50

5.4 Average Nusselt number

The variation in Nu with varying Pr is shown in figure 5.15. The average Nu number is increasing by increasing the Pr at the particular $Re = 7 \times 10^4$. The present results are found in accordance with literature (Askew et al.,1965). The similar trends of average Nusselt number may expected for another values of Reynolds number in the turbulent flow regimes.

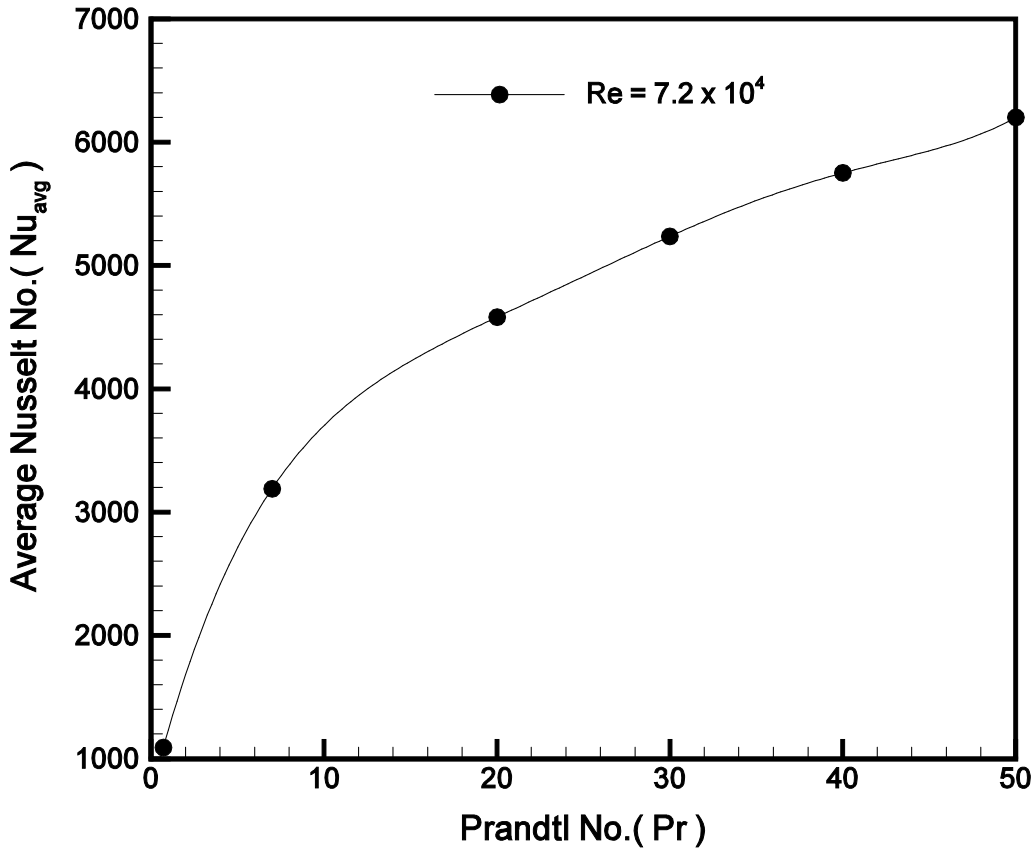


Fig. 5.15 The variation in Nu with Varying Pr

The present results may be correlated and the correlation is presented in equation (11)

$$Y=A+Bx+Cx^2+Dx^3+Ex^4+Fx^5 \quad (11)$$

Where :

$$Y = Nu_{(avg)}$$

x = Prandtl number

$$A=7.188 \times 10^2, B = 5.459 \times 10^2, C= -3.550 \times 10^1, D = 1.2797, E = -2.223 \times 10^{-2}, F = 1.484 \times 10^{-4}$$

CONCLUSION AND FUTURE SCOPE

6.1 CONCLUSION

The following conclusions have been drawn from the present study:

- The numerically predicted results are found to be in good agreement with the experimental data reported in the literature.
- The velocity near the turbine is very high as compare to vessel surfaces in the horizontal plane and in the vertical plane it is maximum below the impeller.
- The tangential velocities are found to be higher than the other two velocities components.
- The pressure was found minimum near the impeller and maximum at cylindrical walls.
- The temperature profile becomes more uniform with the increase in Prandtl number for the same Reynolds number.
- The overall heat transfer also increases with increasing Prandtl number and it shows functional dependency on Prandtl number.

6.2 Future Scope

The present work has been focused on the turbulent heat transfer modeling in an unbaffled, agitated vessel. In addition to this work the following work can be done in future:

- If faster and higher capacity computing facility is available, other model instead of k- can be used to predict the results.
- This numerical simulation can be performed on other fluid.
- The present work can further proceed for helical coil heating in the agitated vessel.
- In the present work unbaffled tank is used, so baffles can be employed to the same geometry.
- The other types of impeller can be used for the same geometry and comparison can be study.

REFERENCES

- Armenante, P.M. & C. C. Chou (1996). "Velocity profile in a single or double Pitched blade turbine." *A.I.Ch.E. J.* 42, 42-54.
- Armenante, P.M., L. Changgen, C. Chou, I. Fort. & J. Medek (1997). "Velocity profiles in a closed, unbaflled vessel: Comparison between experimental LDV data and numerical CFD predictions." *Chem. Eng. Sci.* 52, 3483-3492.
- Aubin, J., D. F. Fletcher & C. Xuereb (2004a). "Modelling turbulent flow in stirred tanks with CFD.", *Therm Fluid Sci.*, 28, 431–445.
- Aubin, J., D. F. Fletcher, & C. Xuereb (2004b). "Modeling turbulent flow in stirred tanks with CFD: The influence of the modeling approach, turbulence model and numerical scheme." *Exp. Therm and Fluid Sci.*, 28(5), 431-445.
- Babu, J. (2010). "Heat transfer studies in agitated vessel using immiscible liquid mixtures" *National Journal on Chem Biosis*, Vol. 1, No. 1.
- Bakker, A., R. D. Laroche, M. Wang & R.V. Calabrese (1997). "Sliding Mesh Simulation of Laminar flow in stirred reactors." *Trans. I.Chem.E.* Vol.75, Part A.
- Bakker, A. & Van Den Akker (1994). "Single-phase flow in stirred reactors", *Trans I.Chem.E* ,72, Part A, 583 - 593.
- Balakrishna, M. & M. S. Murthy (1980). "Heat transfer studies in agitated vessels." *Chem. Engg. Sci.*, Vol. 35, 1486 – 1494.
- Deglon, D. A. & C. J. Meyer (2006). "CFD modeling of stirred tanks Numerical considerations." *Miner. Eng.*, 19, 1059–1068.

- Debab, A., N. Chergui, , K. Bekrentchir, and J. Bertrand (2011). “An Investigation of Heat Transfer in a Mechanically Agitated Vessel.” *Journal of Applied Fluid Mechanics*, Vol. 4, No. 2, Issue 1, 43-50.
- Delaplace, G., C. Torrez, J. C. Leuliet, N. Belaubre & C. Andre (2001). “Experimental and CFD simulation of heat transfer to highly viscous fluids in an agitated vessel equipped with a non standard helical ribbon impeller.” *I.Chem.E*, Vol. 79, Part A, 927 – 937.
- Dong, L., S. T. Johansen & T. A. Engh (1994). “Flow induced by an impeller in an unbaffled Tank -II. Numerical modeling.” *Chem. Engg. Sci.*, Vol. 49, No. 20, 3511 – 3518.
- Driss, Z., G. Bouzgarrou, W. Chtourou, H. Kchaou & M.S. Abid (2010). “Computational studies of the pitched blade turbines design effect on the stirred tank flow characteristics.” *European Journal of Mechanics B/Fluids* 29, 236-245.
- Edwards, M. F. & M. A. Wilkinson (1972). “Heat Transfer in Agitated Vessels, Part I – Newtonian fluids.” *The Chemical Engineer*, 310–319.
- Engeskaug, R., E Thorbjornsen & H. F. Svendsen (2005). “Wall Heat Transfer in Stirred Tank Reactors.” *Ind. Eng. Chem. Res.*, 44, 4949-4958.
- Haam, S., & R. S. Brodkey (1993). “Local Heat Transfer in a Mixing Vessel Using a High Efficiency Impeller.” *Ind. Eng. Chem. Res.*, 32, 575-576.
- Harnby, N., M. F. Edwards & A.W. Nienow (1985). “Mixing in the process industries.” *Butterworths & Co. Ltd.*
- Hockey, R. M. & J. M. Nouri (1996). “Turbulent Flow in a Baffled Vessel Stirred by a 60° Pitched Blade Turbine.” *Chem. Engg. Sci.*, Vol 51, No 19, pp.4405-4421.
- Jorge, M. T., C. P. Vasconcelos, O. Sandra, M. A. F. Ana Rodrigues & S. Sebastia Alves (2000). “Effect of Blade Shape on the Performance of Six-Bladed Disk Turbine Impellers.” *Ind.*

Eng. Chem. Res., 39, 203-213.

Joshi, J. B., N. K. Nere, C. V. Rane, B. N. Murthy, C. S. Mathpati, A. W. Patwardhan, & V. V.

Ranade (2011). "CFD simulation of stirred tanks: Comparison of turbulence models

(Part II: Axial flow impellers, multiple impellers and multiphase dispersions)." *Can. J.*

Chem. Eng., 89, 754–816.

Kaminoyama, M., M. Watanabe, K. Nishi, M. Kamiwano (1999). "Numerical simulation of local

heat transfer coefficients in stirred vessel with impeller for highly viscous fluids."

Journal of Chemical Engineering of Japan, Vol. 32 No. 1, 23-30.

Kumpinskyt, E. (1995). "Heat-Transfer Coefficients in Agitated Vessels. Sensible Heat

Models" *Ind. Eng. Chem. Res.*, 34, 4571-4576.

Karcz, J. & F. Strek (1995). "Heat transfer in jacketed agitated vessels equipped with

nonstandard Baffles." *The Chemical Engineering Journal*, 58, 135-143.

Karcz, J. & K. Lukasz (2012). "An effect of grid quality on the results of numerical simulations

of the fluid flow field in an agitated vessel." *14th European Conference on Mixing*

, Warszawa, 10-13 September.

Kurnpinsky, E (1992). "Experimental determination of overall heat transfer coefficient in

jacketed vessels." *Chem. Eng. Comm.* 115, 13 - 23.

Mohan, P., A. N. Emery & T. Al-Hassan (1992). "Review heat transfer to Newtonian fluids in

mechanically agitated vessels. *Exp. Therm. Fluid Sci.* **1992**, 5 (6), 861-883.

Montante, G., K. C. Lee, A. Brucato, & M. Yianneskis (2004). "Numerical Simulation of the

Dependency of Flow Pattern on Impeller Clearance in Stirred Vessels." *Chemical*

Engineering Science, 56, 3751-3770.

Murthy, J.Y., S.R. Mathur & C. Choudhury (1994). "CFD simulation of flows in stirred tank

- reactors using a sliding mesh technique” *IChemE Symp. Ser.* 136, pp.341–345.
- Nagata, S. (1975). “Mixing: Principles and Applications.” *John Wiley & Sons: Halstead press, Japan.*
- Nagata, S., M. Nishikawa, T. Takimoto, F. Kidaand & T. Kayama (1972). “Turbulent heat transfer from the wall of a jacketed tank.” *Heat Transfer-Japanese Research*, 1 (1), 66 - 74.
- Ochieng, A., M. Onyango, & K. Kiriamiti (2009). “Experimental measurement and computational fluid dynamics simulation of mixing in a stirred tank: A review.” *South African Journal of Science*, 105(11-12), 421-426.
- Oldshue, J. Y. (1983). “Fluid Mixing Technology.” McGraw-Hill, New York.
- Pasquim, B. M. & V. C Mariani (2013). “Numerical Investigation of Internal Flow in Stirred Tanks.” *22nd International Congress of Mechanical Engineerin*, Ribeirao Preto, SP, Brazil, ISSN 2176-5480.
- Patankar, S. V. (1980). “Numerical Heat Transfer and Fluid Flow.” *McGraw Hill, New York.*
- Sahu, K., P. Kumar & J. B. Joshi (1998). “Simulation of Flow in Stirred Vessel with Axial Flow Impeller: Zonal Modeling and Optimization of Parameters.” *Ind. Eng. Chem. Res.*, Vol. 37, pp. 2116 – 2130.
- Wilcox, D. C. (1994). “*Turbulence modeling for CFD*”, DCW Industries, Inc.
- Yang, F. L., S. J. Zhou, C. X. Zhang, G. M. Evans, & G. C. Wang (2013). “Study of the Turbulent Flow in an Unbaffled Stirred Tank by Detached Eddy Simulation.” *Chem. Eng. Comm.*, 200:1347–1365.
- Zakrzewska, B. & Z. Jaworski (2004). “CFD modelling of turbulent jacket heat transfer in a Ruston turbine stirred vessel.” *Chemical Engineering and Technology*, Vol. 27, No. 3, 237-242.